The Lunar Soil

Introduction

The surface of the moon is blanketed by a thin layer of weakly-cohesive detrital materials which is generally referred to as "soil" or "regolith" (Gault et al., 1966; Rennilson et al., 1966; Christensen et al., 1967; Scott et al., 1967; Shoemaker et al., 1967; Cherkasov et al., 1968; Oberbeck and Quaide, 1967; Quaide and Oberbeck, 1968). The soil is a stratified and continuallyevolving sedimentary body produced in large part by hypervelocity meteoroid impact, although locally a pyroclastic volcanic contribution may be present. The understanding of the process by which the lunar soil has accumulated is of particular importance because it may ultimately provide a detailed stratigraphic record of much of lunar history and, in the case of the quiescent post-mare period, it may offer the only stratigraphic record with any continuity. That is, the few meters of lunar soil may offer the only detailed record of in excess of 60 per cent of lunar history. The following chapter is meant to provide some concept of the nature of the lunar soil and an idea of what is currently known of its evolution. The soil evolves in response to poorly understood stochastic processes and as a consequence is difficult to model adequately.

Soil Thickness and Accumulation Rates

Prior to the Apollo missions the thickness of the lunar soil was estimated by studying the geometry of small craters (Oberbeck and Quaide, 1967, 1968; Quaide and Oberbeck, 1968). These estimates proved to be very reliable and still offer the best insight into the variable nature of the soil blanket. Oberbeck and Quaide (1968) found that they could recognize four types of soil thickness distributions, with median thickness values of 3.3, 4.6, 7.5, and 16 meters (Fig. 6.1). The median thickness of the regolith correlates directly with the density of impact craters. The variations in median soil-thickness thus reflect differences in elapsed time since the production of the new rock surface upon which the soil is evolving. The soil

begins as a thin deposit of nearly uniform thickness and gradually changes to a thicker deposit with a greater spread of thickness values. That is, the standard deviation of the soil thickness frequency distribution increases with

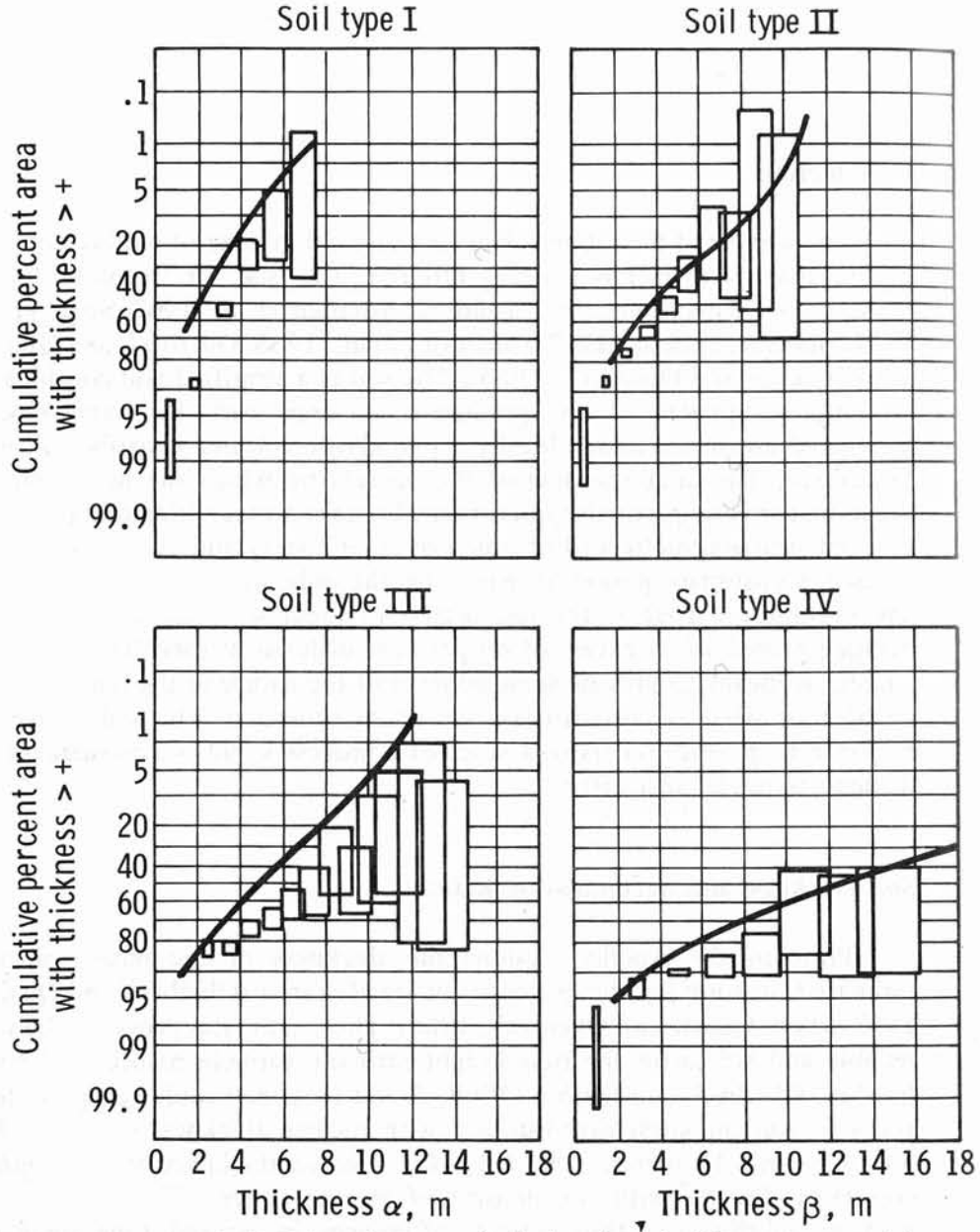


Fig. 6.1. Four observed soil thickness frequency distributions determined from crater morphology (from Oberbeck and Quaide, 1968).

time. The increasing spread of thickness values highlights the stochastic nature of the impact process — soil accumulation is a discontinuous process dependent upon random (in both space and time) hypervelocity impacts.

As a result of the Apollo missions these thickness estimates were, in general, confirmed on the basis of both active and passive seismic experiments (Watkins and Kovach, 1973; Cooper et al., 1974; Nakamura et al., 1975). From these experiments it was concluded that the moon is covered with a layer of low-velocity material that ranges in thickness from between 3.7 and 12.2 m at the Apollo landing sites (Table 6.1). In general the soil thickness increases with the age of the underlying substrate.

Soil accumulation is a self-damping process such that the average accumulation rate decreases with time (Lindsay, 1972, 1975; Quaide and Oberbeck, 1975). If the meteoroid flux had remained constant over time its effectiveness as an agent of erosion would gradually be reduced as the soil blanket grew in thickness. For new material to be excavated from the bedrock beneath the soil an impact must be energetic enough to first penetrate the pre-existing soil layer. As the soil blanket grows, more and more energetic events are required to accomplish the same result. However, returning to Chapter 2, it is evident that the number flux of particles decreases rapidly with increasing particle size and with it the available erosional energy must also decrease. The energy actually available for erosion of bedrock is probably considerably less than 1 per cent of the total meteoritic energy incident on the moon (Lindsay, 1975) (Fig. 6.2). Whatever the history of bombardment there should be rapid initial accumulation of soil followed, by gradually decreasing growth rates.

Modelling of such complex processes requires more knowledge than is currently available about the meteoroid flux, and therefore some simplifying

TABLE 6.1

Estimates of regolith thickness based on seismic data from each of the Apollo landing sites (data from Nakamura et al., 1975).

Apollo Station	Thickness (m)	Minimum Age of Substrate (x 109 yr)
11	4.4	3.51
12	3.7	3.16
14	8.5	3.95
15	4.4	3.26
16	12.2	-
17	4.0, 8.5	3.74

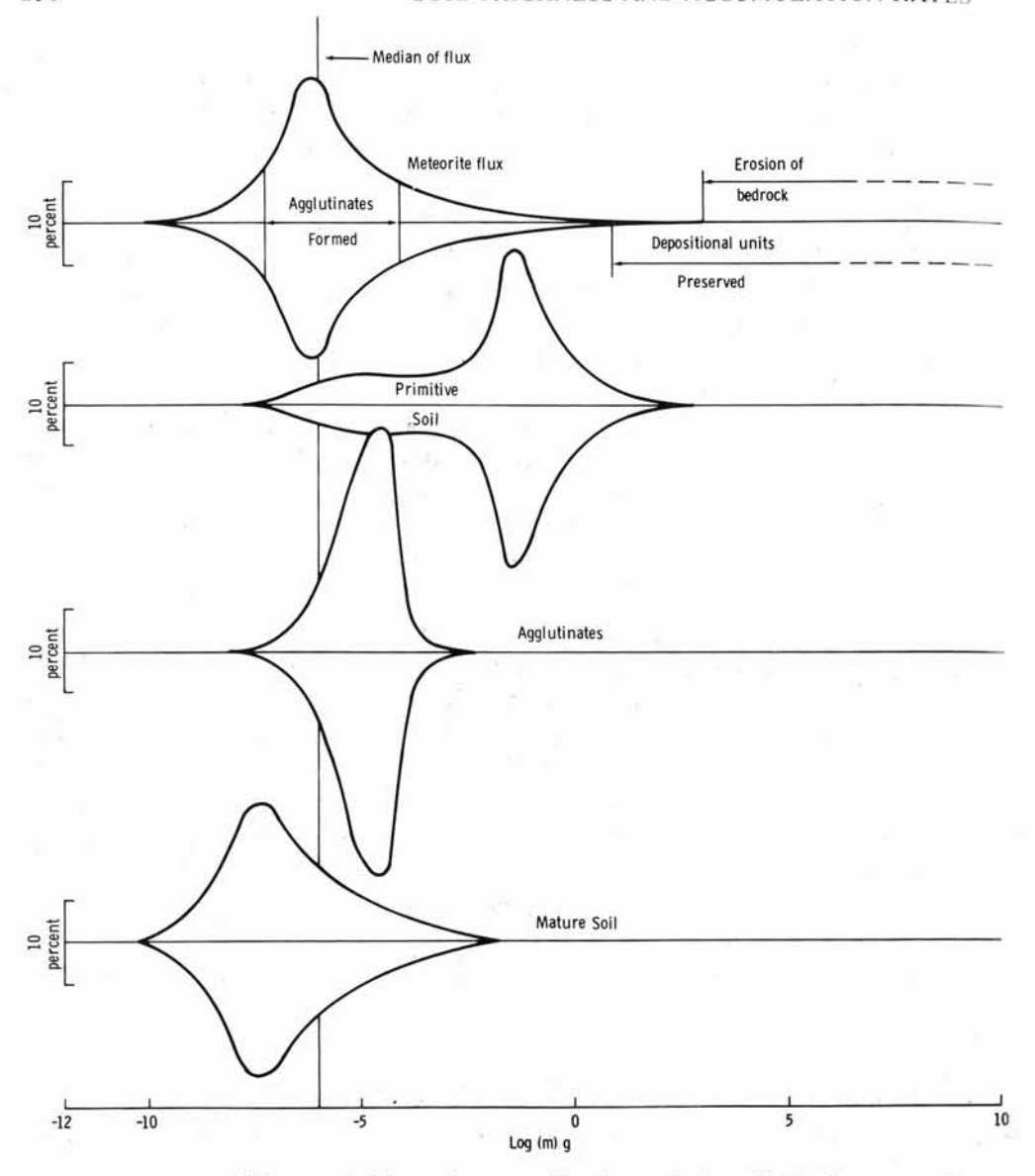


Fig. 6.2. The meteoroid flux, a primitive and mature soil and an agglutinate distribution expressed as weight per cent per decade of mass. Note the similar shape of the meteoroid flux distribution and the lunar soil (from Lindsay, 1975).

assumptions are necessary. Quaide and Oberbeck (1975) have used a Monte Carlo approach to study average cases of soil growth on mare surfaces. If the meteoroid flux has been constant since the flooding of the mare the thickness (Th) of the soil blanket is related to its age (A) by

$$Th = 2.08 A^{0.64}$$
 (6.1)

where Th and A are in meters and aeons respectively. The accumulation rate (dTh/dA) decreases exponentially with time (Fig. 6.3). This observation has considerable bearing on the understanding of the texture and mineralogy of the soil. As the accumulation rate declines more and more of the kinetic energy of the meteoroid flux is redirected into mixing and reworking the soil. This extra energy is particularly important in modifying the grain-size parameters of the soil which in turn affects the nature of the impact-produced glass particles and the glass content of the soil. Because smaller volumes of fresh bedrock material are added with time, any materials that are cumulative will increase in concentration — this is true of impact glasses (Lindsay, 1971a, 1972c) and should be true of the meteoritic materials themselves.

Soil Stratigraphy and Dynamics

The lunar soil is layered. This observation was first made in drive-tube core samples returned by Apollo 12 (Lindsay *et al.*, 1971) and has since been confirmed in deeper drill cores collected by subsequent Apollo missions (Heiken *et al.*, 1973; Duke and Nagle, 1975) (Fig. 6.4).

The Apollo 15 deep drill core intersected 42 major stratigraphic units and a large number of sub-units ranging from 0.5 cm to 20 cm in thickness (Heiken et al., 1973). The thickness-frequency distribution of the units is

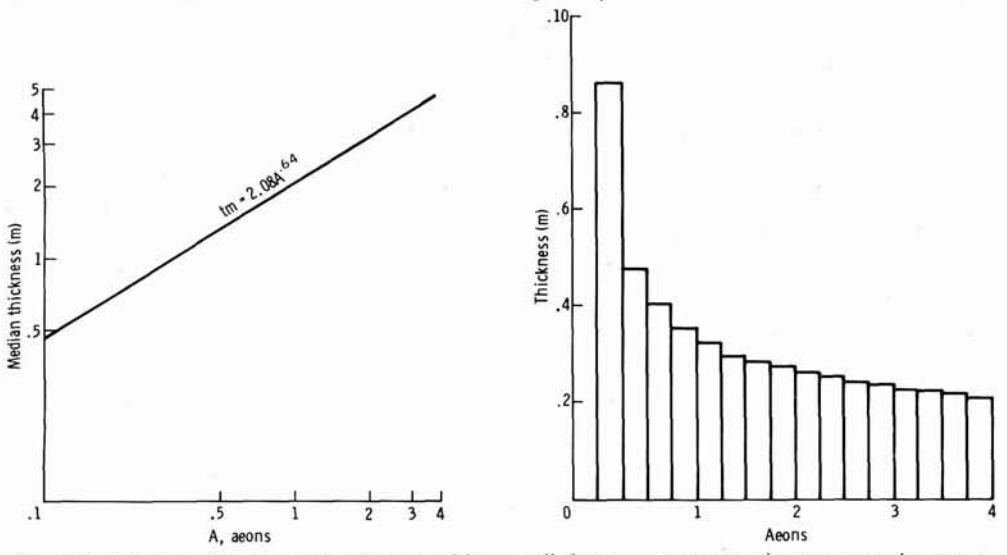


Fig. 6.3. Accumulation rate and thickness of lunar soil for a constant cratering rate over 4 aeons. The accumulation rate is damped exponentially by the gradually thickening soil blanket (after Quaide and Oberbeck, 1975).

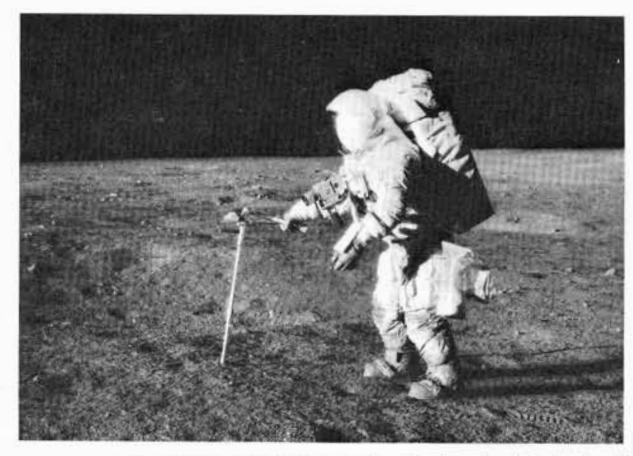


Fig. 6.4. Sampling the lunar soil with a drive tube during the Apollo 12 mission (NASA Photo AS12-49-7286).

bimodal with the strongest mode at 1.0 to 1.5 cm and a secondary mode at 4.5 to 5.0 cm (Fig. 6.5) (Lindsay, 1974). Preliminary analysis of drill-core samples from the Apollo 16 landing site suggests that this distribution may be typical of the lunar soil (Duke and Nagle, 1975).

The units are distinguished on the basis of soil color and texture, particularly variations in grain size. The contacts of the units are generally sharp, although at times difficult to observe because the textural differences are subtle. Some units have transitional contacts and structures similar to flame structures were observed at the base of other units. Both normal and reverse graded beds have been described (Lindsay *et al.*, 1971; Heiken *et al.*, 1972; Duke and Nagle, 1975).

The presence of normal and reverse graded bedding in the lunar soil (Lindsay et al., 1975; Heiken et al., 1972; Duke and Nagle, 1975) suggests that a single set of depositional processes were operative during the formation of at least some stratigraphic units. Grain size data from individual units suggests that two processes may be active in the transport of soil materials following a hypervelocity impact, i.e. base surge and grain flow (Lindsay, 1974). Both of these processes are discussed in detail in Chapter 3.

An impacting meteoroid, by virtue of the heat energy generated, may produce large volumes of gas and a base surge may develop. Detrital particles transported in a base surge are fluidized by the upward flow of escaping gases. The settling velocity (under Stokes Law) of the particles is determined by their size and to some extent their shape. Consequently, larger and more spherical particles tend to move towards the base of the fluidized flow and produce a normally-graded detrital mass. However, the supply of fluidizing gases is not necessarily in any direct proportion to the size or velocity of the

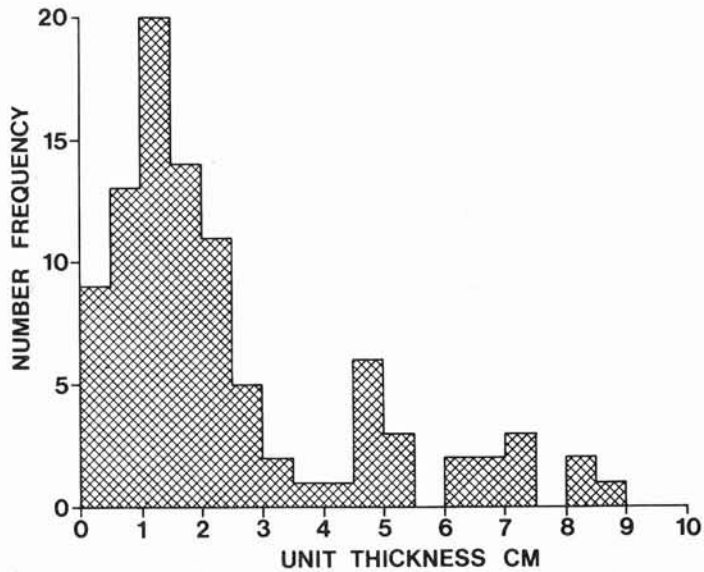


Fig. 6.5. Thickness frequency distribution of soil units intersected by a deep drill core at the Apollo 15 site. The distribution is unexpectedly bimodal (after Lindsay, 1974).

flowing mass, with the result that one of two things can happen. If the gas supply is abundant fluidization may continue until the flow loses momentum and comes to rest as a normally-graded depositional unit. If on the other hand, the gas supply is limited fluidization may cease before the flow has completely come to rest. In this case inertial grain flow will dominate. During inertial grain flow a dispersive pressure is generated which causes larger particles to migrate upwards through the flow to the region of least shear strain resulting in a reverse-graded bed. Some depositional units show the effects of both in that larger particles concentrate in the middle of the unit (Lindsay, 1974) (Fig. 6.6). Similar sorting effects are also apparent in particle shape studies where more spherical particles are found to congregate in the middle of the depositional unit (Lindsay, 1974) (Fig. 6.7).

While it is reasonable to suggest that at least some strata in the lunar soil are formed by single impact events, it is by no means clear that all strata have such simple origins (Fig. 6.8). Hypervelocity cratering experiments suggest that an inverted stratigraphy may be preserved in the ejecta blankets of successive cratering events (see Chapter 3 for details). If so, the lunar soil may be a complex of first generation units interbedded with inverted sequences of older generation depositional units. Evidence of inverted sequences is limited. Recently however, Gose et al. (1975) have found systematic changes in the magnetic properties of the Apollo 15 core which they interpret as evidence of stratigraphic inversions. The evidence is however ambiguous and the deviations may be explained by other causes.

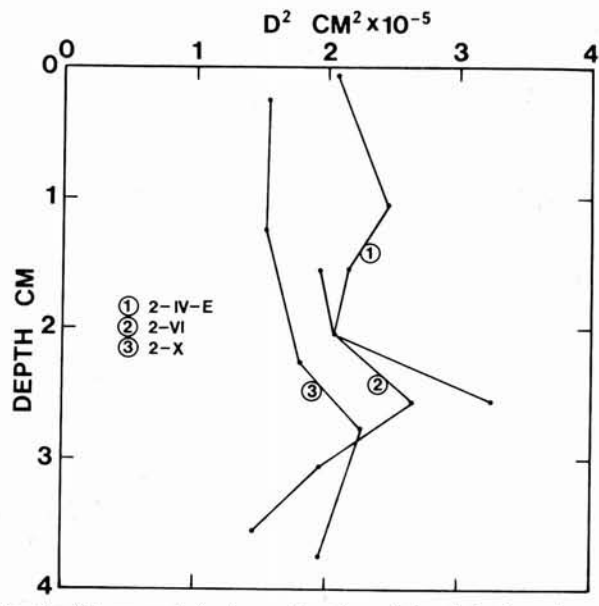


Fig. 6.6. Mean grain size (D) squared (cm) as a function of depth in three lunar soil layers from the Apollo 15 deep drill core (after Lindsay, 1974). Larger particles tend to concentrate in the middle of the units.

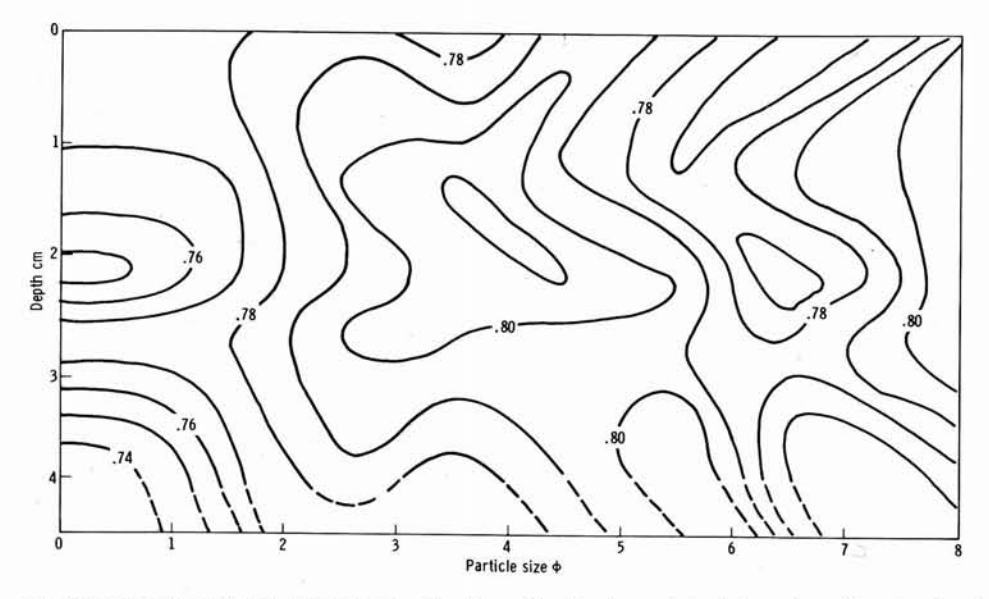


Fig. 6.7. Two dimensional sphericity as a function of grain size and depth in a depositional soil unit from the Apollo 15 deep drill core. The more spherical particles tend to concentrate in the middle of the unit (after Lindsay, 1974).



Fig. 6.8. A small crater in lunar soil surrounded by a thin ejecta blanket. The crater has not penetrated the soil blanket but has simply redistributed the soil to produce a new stratigraphic unit which may or may not survive subsequent reworking (NASA Photo AS15-85-11466).

Whether or not stratigraphic inversions exist, there is clear evidence that some depositional units are reworked by micrometeoroids. For example, if each unit is a depositional unit we could expect the thickness-frequency distribution in Figure 6.5 to reflect, in some simple way, the meteoroid flux. That is, the number of units should increase exponentially as the unit thickness decreases. However, in both cores so far studied this is not the case, the number frequency peaks then declines sharply (Lindsay, 1974; Duke and Nagle, 1975). Very thin depositional units are thus either not formed or are destroyed by reworking. In most of the lunar cores evidence of such reworking can be observed directly. For example, some strata consist of dark soil with rounded clods of lighter soil included within them, somewhat similar to a mudchip breccia. Duke and Nagle (1975) call this texture an "interclastic soil chip breccia." The clods or soil chips are no more cohesive than the matrix soil. Since the clods occur only near the upper contact of the unit it seems most likely that we are looking at an incompletely homogenized compound unit. A thin layer of light soil apparently overlay a thicker dark soil unit, and the clods are the incompletely mixed remnants of the thin layer of light soil. Undoubtably, many other thin units of soil have been reworked in the same way but are not visible because thay lack distinctive physical properties or were completely homogenized. Many fresh glass particles show a selenopetal (lunar geopetal) orientation, related to depositional configuration (Duke and Nagle, 1975). These glass splashes struck the lunar surface while hot, outgassed and vesiculated on their upper surfaces and incorporated dust into their bases. Such glass particles in many 236 SOIL DENSITY

units indicate that they are still undisturbed and in their depositional configuration. In some units however, the particles are overturned and fractured indicating reworking. There is no evidence of overturned sequences from selenopetal structures.

Probabilistic models for mixing and turnover rates due to hypervelocity impact suggest that the upper millimeter of the lunar soil is the primary mixing zone (Fig. 6.9) (Gault et al., 1974). This mixing zone is probably coincident with the zone in which agglutinates form. Agglutinates are complex constructional glass particles and are discussed in a following section (p. 261). Below this mixing zone the rate of turnover and mixing decreases very rapidly with increasing depth which explains the well-preserved soil stratigraphy.

Soil Density

The mean density of the particulate material forming the lunar soil ranges from 2.90 to 3.24 g cm⁻³ depending upon the nature of source materials. Basaltic mare soils tend to be denser than the more anorthositic highland soils. It has been found experimentally that the porosity of lunar soils may range from 41 to 70 per cent with the result that soil density is variable (Carrier *et al.*, 1974). The main reason for the range in porosities is probably connected with the abundance of extremely-irregularly-shaped

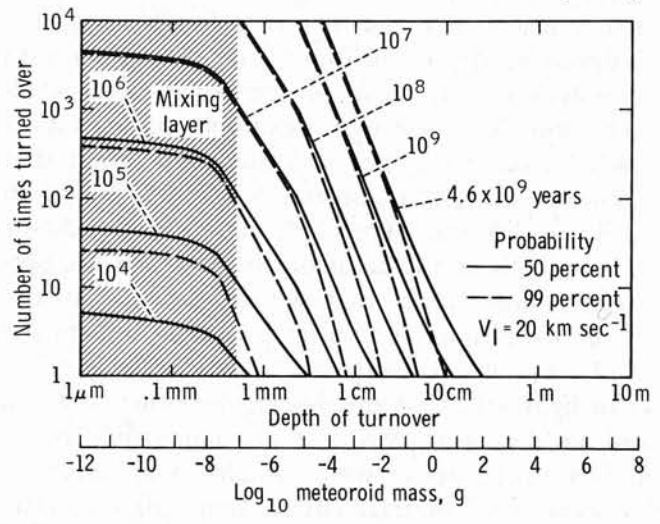


Fig. 6.9. A probabilistic model for soil reworking based on a constant meteoroid mass flux. The number of times the soil is turned over is shown as a function of depth and time. Most reworking occurs in a millimeter surface zone where agglutinates are formed (from Gault et al., 1974; Proc. 5th Lunar Sci Conf., Suppl. 5, Vol. 3, Pergamon).

glass particles (agglutinates) which are discussed in a following section. Data from core tubes driven into the lunar surface have shown that soil density increases in a logarithmic manner with depth (Carrier *et al.*, 1974). The density profile can be approximated by

$$\rho = \rho_0 + 0.121 \ln (Z + 1) \tag{6.2}$$

where ρ_0 and ρ are the density at the surface and at some depth Z (cm). ρ_0 is approximately 1.38 g cm⁻³ at the Apollo 15 site. The continual reworking of the lunar surface apparently keeps the surface layers of the soil loose but at depth the vibration due to the passage of numerous shock waves causes the soil to increase in density.

Composition of Lunar Soils

The chemistry and mineralogy of the lunar soils, for the most part, reflect the composition of the underlying bedrock (Table 6.2). Thus soils from mare areas have an overall basaltic composition with a high Fe content, while the highland soils tend to be more anorthositic in composition and

TABLE 6.2

Major element chemistry of average Apollo 15 soils and basalts. There is a general similarity between the soils and basalts but the higher Al₂O₃ value of the soils indicates the addition of some highland materials (after Taylor, 1975).

	Average Soil	Olivine Basalt	Quartz Basalt
SiO ₂	46.61	44.2	48.8
TiO_2	1.36	2.26	1.46
Al_2O_3	17.18	8.48	9.30
FeO	11.62	22.5	18.6
MgO	10.46	11.2	9.46
CaO	11.64	9.45	10.8
Na ₂ O	0.46	0.24	0.26
K ₂ O	0.20	0.03	0.03
P_2O_5	0.19	0.06	0.03
MnO	0.16	0.29	0.27
Cr_2O_3	0.25	0.70	0.66
TOTAL	100.13	99.46	99.08

have high Al and Ca values (Table 6.3). It has been estimated that, in general, 95 per cent of a soil sample at any given point on the moon is derived from within 100 km (Fig. 6.10) (Shoemaker et al., 1970). The proportion of exotic components decreases exponentially with distance. Orbital chemical data further emphasize the local derivation of the bulk of the soil. Secondary X-rays generated at the lunar surface by primary solar X-rays allow a determination of Al, Mg, and Si (Adler et al., 1972a, 1972b). The secondary X-rays are generated in the $10~\mu m$ surface layer and thus offer a good picture of the lateral distribution of the lunar soil with a spatial resolution of about 50 km. In Figure 6.11 it can be seen that in general high Al/Si values coincide with highland areas and low values coincide with the mare areas. The boundaries between the two are sharp at the available resolution. Lateral movement of detrital material thus cannot be rapid despite continued reworking for long time periods by the meteoroid flux.

Soil Petrography

The lunar soil consists of three basic components: (1) rock fragments, (2) mineral grains and (3) glass particles. The composition of these three basic components varies considerably from one site to another, depending upon the nature of the bedrock. They also vary in abundance laterally and with depth in the soil in response to the addition of more distant exotic components, the degree to which the soil has been reworked (its age), and in response to bedrock inhomogeneities (Table 6.4).

TABLE 6.3

Average major element chemistry for highland and mare soils (after Turkevich et al., 1973).

		Per cent of ato	ms	Weight per cent of oxides			
Element	Mare	Highland	Average surface	Mare	Highland	Average surface	
О	60.3 ± 0.4	61.1 <u>+</u> 0.9	60.9				
Na	0.4 ± 0.1	0.4 ± 0.1	0.4	0.6	0.6	0.6	
Mg	5.1 ± 1.1	4.0 ± 1.1	4.2	9.2	7.5	7.8	
Al	6.5 ± 0.6	10.1 ± 0.9	9.4	14.9	24.0	22.2	
Si	16.9 ± 1.0	16.3 ± 1.0	16.4	45.4	45.5	45.5	
Ca	4.7 ± 0.4	6.1 ± 0.6	5.8	11.8	15.9	15.0	
Ti	1.1 ± 0.6	0.15 ± 0.08	0.3	3.9	0.6	1.3	
Fe	4.4 ± 0.7	1.8 ± 0.3	2.3	14.1	5.9	7.5	

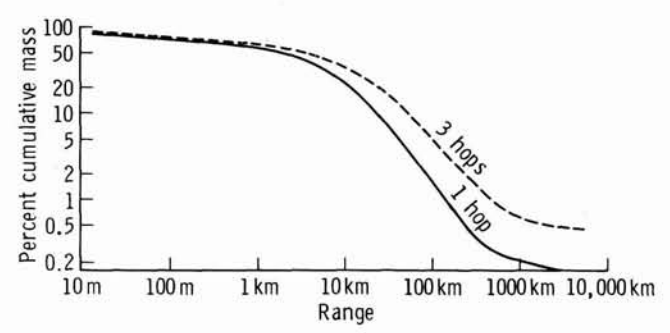


Fig. 6.10. Dispersion of detrital soil materials by impact cratering. Most soil materials are locally derived (after Shoemaker et al., 1970; Proc. Apollo 11 Lunar Sci. Conf., Suppl. 1, Vol. 3., Pergamon).

Lithic Clasts

Lithic clasts are the dominant component in particle size ranges larger than 1 mm (60 to 70 per cent of the 1-2 mm size range). Below 1 mm their importance decreases rapidly as they are disaggregated to form mineral and glass particles. The coarser the mean grain size of the soil the greater, in general, the abundance of lithic fragments.

Three categories of clastic fragments should be considered (1) igneous rock fragments, (2) crystalline breccias and (3) soil breccias.

Igneous Rock Clasts

Mare basalts with the full range of textures are by far the most common igneous lithic fragment and dominate the soils at the mare sites. At the highland sites some igneous rock fragments are encountered but most of them appear to be reworked clasts from the underlying crystalline breccia bedrock. Most of these clasts consist of plagioclase grains and come from grabbroic-noritic-anorthositic sources or, less frequently, from a highland basalt source. Small numbers of feldspathic-lithic fragments occur in the mare soils, providing the first indication of the composition of the lunar crust (Wood *et al.*, 1970). Because the grain size of the minerals is large compared to the size of the clasts, positive identification of many lithologies is difficult. More complete information is available from the chemistry of homogeneous impact melt glasses which is discussed in a following section.

Crystalline Breccia Fragments

Crystalline breccia fragments dominate the lithic clasts in all of the highland soils. They are bedrock fragments derived from units such as the Fra Mauro and Cayley Formations. Fragments of all of the matrix types are represented but again, because of the size of the clasts in relationship to the grain size of the detrital materials forming the breccias, it is not possible to

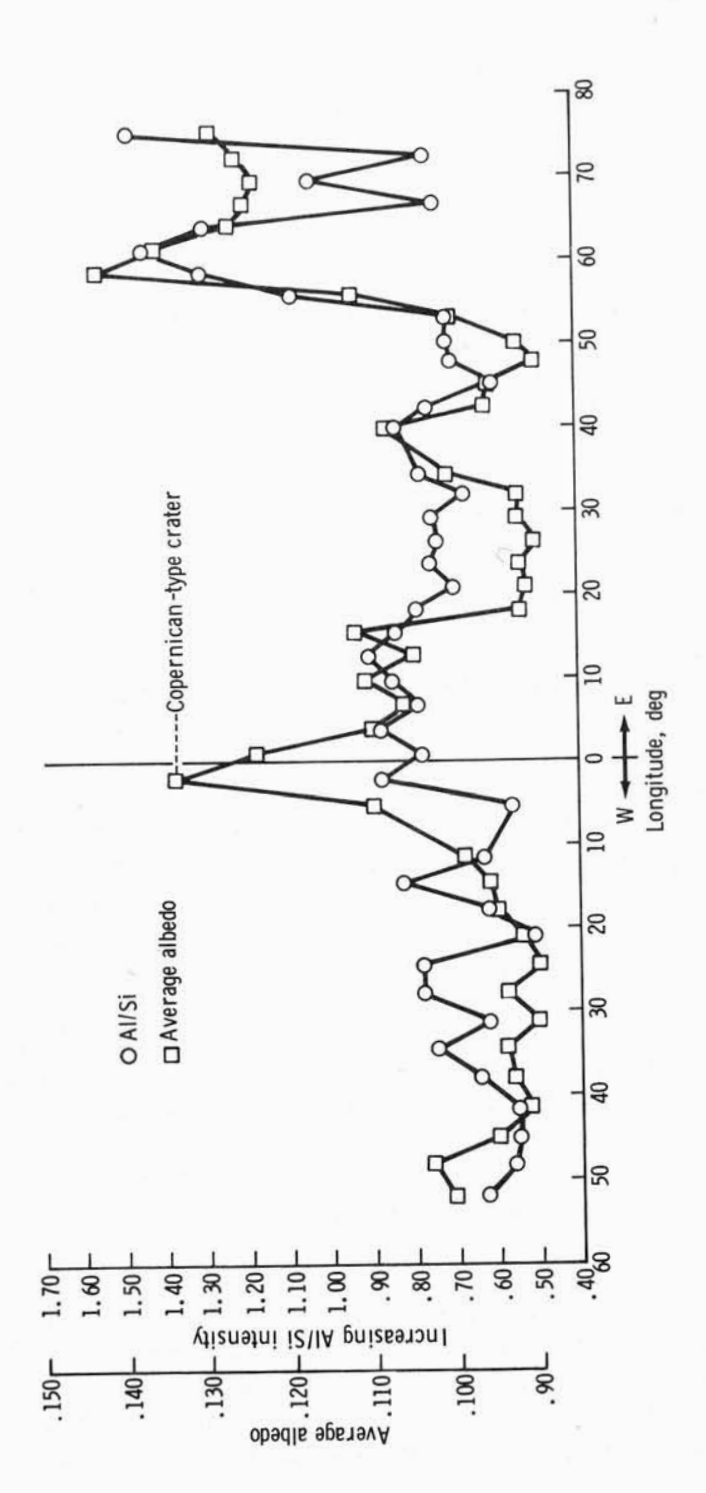


Fig. 6.11. Comparison of Al/Si ratios from the orbital x-ray fluorescence experiment with albedo for a single revolution of the moon. Note that in general the two variables are sympathetic and the highland mare transition is very abrupt indicating little lateral dispersal of soil (from Adler et al.,

TABLE 6.4

Comparison of the modes of the 90 to 150 μ m fraction of a range of soils from the Apollo 14 site. Coarse grained soils contain few agglutinates (adapted from McKay et al., 1972).

Components					14230,	14230,	14230,	
	14259	14148	14156	14149	113	121	130	14141
	Surface	Trench	Trench	Trench	Core	Core	Core	Cone
co	mprehens	ive top	middle	bottom	Sta. G	Sta. G	Sta. G	Crater
	samples	(Sta. G)	(Sta, G)	(Sta, G)	(-8.0 cm)	(-13.0 cm)	(-17.0 cm)	surface
Agglutinates	51.7	50.2	47.7	26.4	53.2	57.0	51.5	5.2
Breccias								
Recrystallized	20.3	24.2	23.4	27.0	13.5	16.3	27.0	49.5
Vitric	5.0	4.6	-	8.2	_	4.3	0.4	7.8
Angular Glass Fr	agments							
Brown	6.7	6.0	7.8	6.0	8.4	7.3	5.2	7.6
Colorless	3.3	2.4	3.2	2.8	1.9	3.0	0.4	2.6
Pale Green	-	0.8	0.9	$\tilde{a} \rightarrow \tilde{a}$	-	1.3	0.9	177
Glass Droplets								
Brown	1.3	1.8	3.2	1.6	4.8	0.3	2.6	2.0
Colorless	0.6	-	0.4	2.0	-	-	-	0.2
Pale Green	0.3	0.2	1.5	0.4		-	-	-
Clinopyroxene	3.7	1.8	4.3	7.4	6.8	3.0	3.0	8.0
Orthopyroxene	0.6	1.4	1.3	3.6	0.6	0.6	-	3.8
Plagioclase	4.7	3.0	5.4	7.8	6.5	3.3	3.4	7.6
Olivine	100	0.8	0.2	-	0.6	-	0.4	0.4
Opaque Minerals	-	0.4	0.4	0.4	-100	-	22	0.4
Ropy Glasses	0.6	0.2	0.2	1-2	2.9	1.7	2.1	-
Basalt	1.0	2.0	_	6.4	0.3	1.6	2.1	4.2
No. of Grains			2					
Counted	300	500	500	500	300	300	234	500

evaluate the relative abundance of different lithologic types.

Soil Breccias

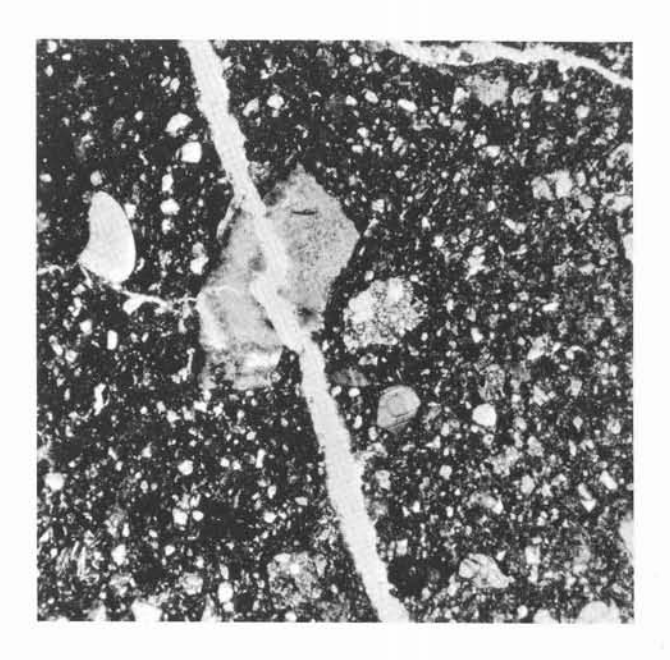
Soil breccias are impact-lithified breccias formed directly from the lunar soil. The coarser grain size fractions of all lunar soils include a large proportion of soil breccia fragments. The soil breccias are particularly important in the evolution of the soil because like agglutinates they are constructional particles.

Soil breccias are poorly sorted agglomerations of rock, mineral and glass fragments which to a large extent preserve the texture of the parent soil. They are characterized by a very open discontinuous framework and are estimated to have a void space of about 35 per cent. The breccias have densities of around 2 g cm⁻³ which is only slightly greater than unconsolidated soil (Waters *et al.*, 1971; McKay *et al.*, 1970). The spaces between the larger clasts of the framework are filled with glass-rich clastic materials with an average grain size of about 50 μ m (i.e. close to the mean grain size of typical lunar soils). The glass forming this matrix tends to be well sorted, closely

fitted and plastically molded against the larger clastic rock fragments. In a general way the texture of these rocks resembles terrestrial ignimbrites (Waters et al., 1971), but contrasts sharply with the texture of shock-lithified materials from chemical explosions (McKay et al., 1970). Glass fragments exhibit a wide variety of devitrification features, ranging from incipient to complete devitrification.

There are two prominent textural features of the soil breccias which provide insights into their despositional history: (1) layering and (2) accretionary lapilli. Very-weakly-defined layering or bedding is seen in many of the soil breccias, generally in the same samples where accretionary lapilliare abundant (Waters et al., 1971; Lindsay, 1972). Accretionary lapilli are present in soil breccias from all of the Apollo landing sites and appear to be an intrinsic characteristic of the lithology (McKay et al., 1970, 1971; Lindsay, 1972a, 1972b). The accretionary structures range in size from 50 μ m to 4mm and at best are weakly defined (Fig. 6.12). In some samples they form complex aggregates of several lapilli. Some aggregates have an outer accretionary layer surrounding the entire structure. The lapilli generally have a core of one or more larger detrital grains which appear to have acted as a nucleus as the structure accreted. The core is surrounded by alternating layers of dark fine-grained glassy material and of larger detrital grains. The shape of the accretionary layers changed as the lapillus developed. Layers may pinch out or the shape may be changed suddenly by the incorporation of a large detrital grain or another lapillus. Most lapilli are roughly circular or ovoid in section. They are generally similar to terrestrial volcanic accretionary lapilli except that the layering is much more weakly defined (Moore and Peck, 1962).

Genesis of Soil Breccias. The texture of the soil breccias suggests that they have originated, not by direct shock lithification due to meteoroid impact, but in a base surge generated by such an impact. The accretionary lapilli may have formed in turbulent areas of the hot base surge or in the impact cloud which later forms the fall back (McKay et al., 1970). The low density of the breccias and the draping of matrix glass around larger clasts suggests that lithification results from sintering. At the time of sintering the breccias were heated to the yield temperature of the finest glass fraction. Without an atmosphere sintering proceeds at a much lower temperature than in the terrestrial environment and in the absence of pressure the nature of breccias formed by viscous sintering becomes very time and temperature dependent (Uhlmann et al., 1975; Simonds, 1973). An analysis of the kinetics of sintering has delineated several regions in which breccia types should form (Uhlmann et al., 1975) (Fig. 6.13). In the first region amorphous matrix breccias form in very short time intervals. Time is sufficient for matrix



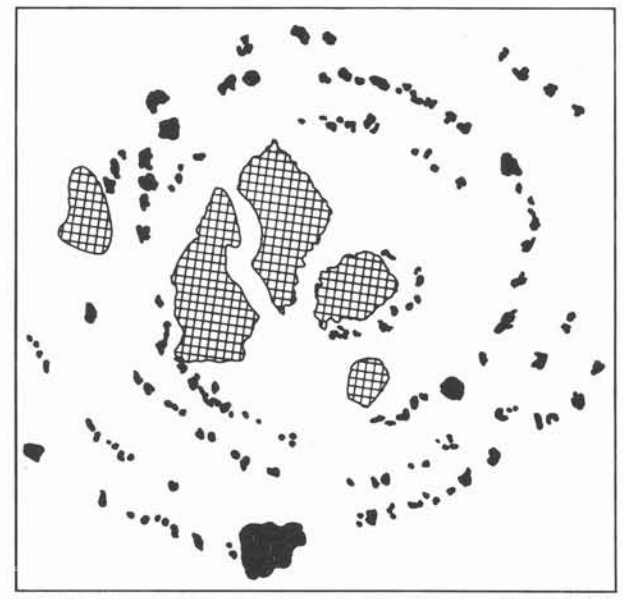


Fig. 6.12. An accretionary lapillus in a soil breccia from the Apollo 14 landing site. Larger detrital grains form the core of the lapillus. The lapillus is approximately 1 mm in diameter (NASA Photo S-71-30835).

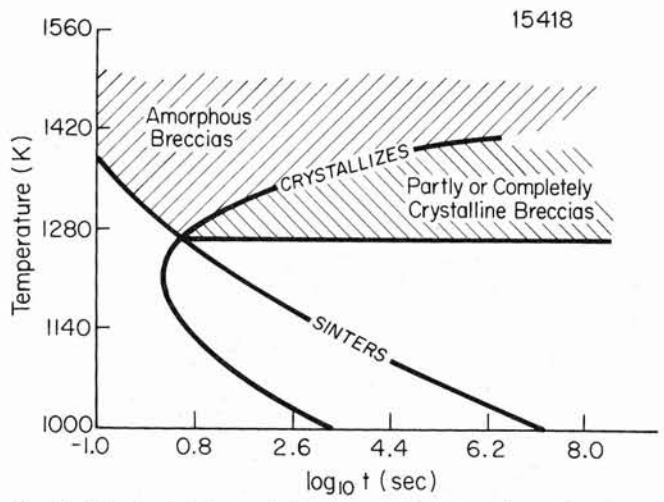


Fig. 6.13. Curve for significant sintering and time-temperature-transformation curve corresponding to a just-detectable degree of crystallinity for Lunar Composition 15418. Regions indicate where amorphous breccias and breccias with detectable crystallinities are formed (from Uhlmann *et al.*, 1975).

sintering to occur but not sufficient for any significant crystallinity to develop. In the second region partly or completely crystalline breccias develop due to the increased time available. In the third region (unshaded in Fig. 6.13) breccias do not form because there is insufficient time for sintering to occur or the materials will crystallize before significant sintering can occur.

Maturity of Soil Breccias. The mineralogic maturity of a sedimentary rock is a measure of the total energy involved in its formation. The main energy source on the lunar surface is the meteoroid flux. In the case of the lunar soil energy from successive impacts is released through (1) vitrification and (2) comminution. A mature soil breccia should, therefore, contain an abundance of glass and an abundance of fine-grained detrital material most of which is glass (i.e. matrix material). The proportion of glass plus matrix material can thus be used as a practical measure of maturity for soil breccias.

Maturity is probably most readily visualized in the form of a ternary diagram with end members of (1) glass plus matrix (defined for practical purposes here as $<15 \mu m$) (2) mineral fragments and (3) lithic clasts (Fig. 6.14). Most of the samples cluster relatively tightly near the glass plus matrix apex indicating generally very-mature detrital materials. The soil breccias thus probably formed from soils which had evolved in a regular manner with a few introductions of coarse impact-derived bedrock materials. It also suggests that the events which formed the breccias were probably not large enough themselves to excavate bedrock but simply sintered existing soil. Only five samples lie beyond the main cluster and closer to the lithic apex.

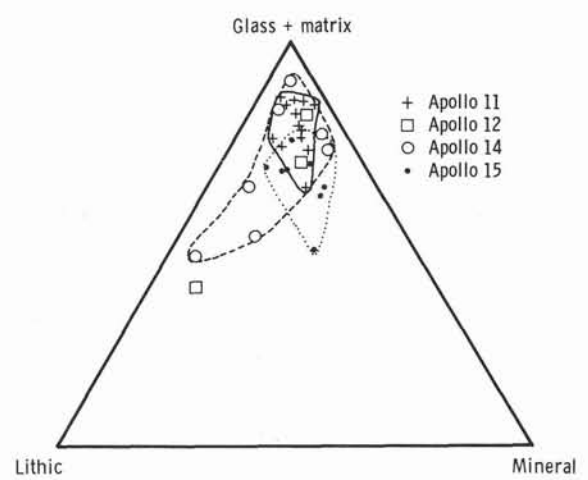


Fig. 6.14. Ternary diagram showing the relative maturity of soil breccias from several Apollo landing sites. Apollo 11 field, solid line; Apollo 14 field, dashed line; and Apollo 15 field, dotted line (after Lindsay, 1972b).

The anomalous Apollo 14 sample can be associated with coarse soils excavated from Cone Crater, and the anomalous Apollo 15 breccia may come from Elbow Crater.

Grain Size of Soil Breccias. Soil breccias are relatively fine grained which, combined with the difficulty of identifying small sintered glass particles and agglutinates, makes grain size determinations difficult. Lindsay (1972a, 1972b) attemped to determine the grain-size distribution of soil breccias using thin section data and Friedman's (1958; 1962) conversions to determine sieve size equivalents. In general the mean grain sizes determined in this way are consistently much finer than equivalent soils from the same site (Table 6.5). This suggests two possibilites: (1) it is not possible to identify agglutinates in thin sections and they are being analysed in terms of their detrital components or (2) because soil breccias are formed from the soil by larger impact events many or most agglutinates are destroyed during crater

TABLE 6.5

Grain size of lunar soil breccias (from Lindsay, 1972b).

Mission	Mean Median		Number of Samples	
	φ	μm		
11	5.99 ± .0	61 15.7	14	
12	4.20	54.4	3	
14	4.75 ± 1.7	76 37.2	7	
15	5.14 ± 1.0	00 28.4	11	

excavation. Detailed thin section analysis of the breccias combined with skewness data from the soils suggests that many agglutinates are destroyed by larger layer-forming impact events.

Regardless of the true grain size of the soil breccias the measured grain size varies sympathetically with the grain size of the local soils. This effect is particularly noticeable in the vicinity of larger craters which penetrate to bedrock and produce coarser soil breccias at the Apollo 14 site all come from the vicinity of Cone Crater. Similarly at the Apollo 15 site the coarse-grained breccias come from the rim of Dune Crater and from close to Elbow Crater both of which penetrate the soil blanket. As with the petrographic data this again emphasises the extremely local nature of the soil breccias.

Roundness of Detrital Grains in Soil Breccias. Communition is the main process by which the morphology of detrital soil particles is modified. As a consequence mineral grains incorporated into the soil breccias are generally very angular (Table 6.6). With the exception of breccia samples from the Apollo 14 site, plagioclase and pyroxene grains have roundness value of between approximately 0.1 and 0.2 resulting in small roundness sorting values. These values are almost certainly determined by the mechanical properties of the minerals themselves.

The effects of communition on roundness are best illustrated by the Apollo 14 soil breccias. The clastic rocks of the Fra Mauro Formation contain moderately-well-rounded plagioclase grains (up to 0.6, see Chapter 5). The soils and soil breccias are derived from the Fra Mauro Formation and inherit many of these comparatively (by lunar standards) well-rounded grains (Fig. 6.15). Continued reworking of the soils by the micrometeoroid flux gradually reduces them to smaller angular grains. Consequently, when the mean roundness of plagioclase grains is plotted as a function of the maturity of the breccia, a strong negative linear dependence can be seen (Fig. 6.16). That is, as more energy is applied to the reworking of the original soil, the

TABLE 6.6

Mean roundness values for plagioclase grains from lunar soil breccias. A minimum of 50 grains (100 to 200 µm in diameter) were measured for each sample (data from Lindsay, 1972b).

Mission	Grand Mean Roundness	Grand Mean Roundness Sorting	Number of Samples
11	$0.197 \pm .031$	0.100 ± .015	14
12	0.243	0.135	3
14	$0.242 \pm .055$	$0.114 \pm .008$	7
15	$0.175 \pm .021$	$0.090 \pm .019$	11

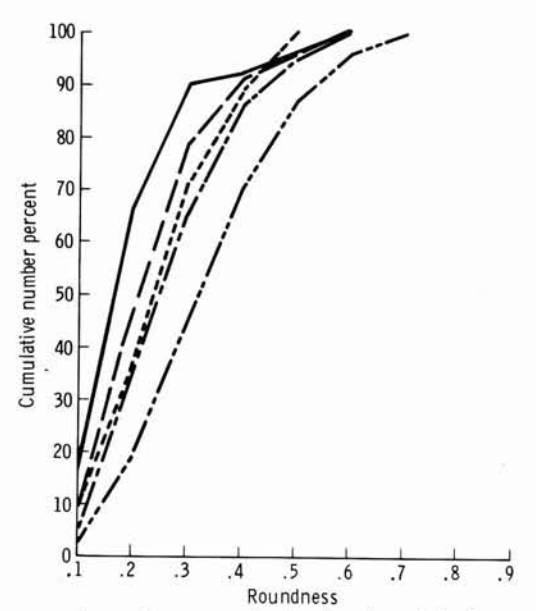


Fig. 6.15. Cumulative roundness—frequency distribution for plagioclase grains from Apollo 14 soil breccias (after Lindsay, 1972a).

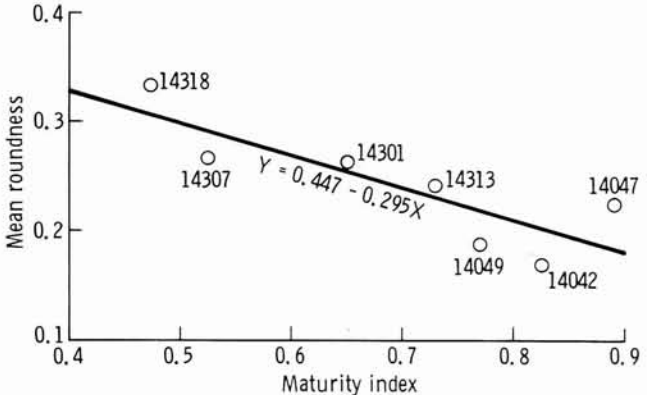


Fig. 6.16. Mean roundness of plagioclase grains from Apollo 14 breccias plotted as a function of maturity. Mean roundness decreases with increasing maturity due to comminution of detrital grains with large inherited roundness values (after Lindsay, 1972b).

mean roundness of the plagioclase grains is reduced by comminution (Lindsay, 1972a, 1972b).

Mineral Grains in Soils

Mineral grains are the dominant detrital particles in the intermediate grain sizes, particularly between 3ϕ (62.5 μ m) and 4ϕ (32.1 μ m) on the coarse side of the mean grain-size of the bulk soil (Table 6.7). This distribution probably reflects the grain size of the source rocks to a large extent although the physical properties of the minerals themselves are also important.

As is the case for lithic fragments the detrital mineral grains present in a soil reflect, for the most part, the nature of the underlying bedrock. The grains are generally highly angular except at the Apollo 14 site where moderate degrees of roundness are inherited from the source materials. Most mineral grains, but particularly the plagioclases, show much evidence of TABLE 6.7

Modal composition of two highland soils from the Apollo 14 site. Sample 14141 is a coarse grained texturally immature soil with finer agglutinates whereas sample 14003 is fine grained, texturally mature and contains an abundance of agglutinates (adapted from McKay et al., 1972).

Components		1414	1,30		14003,28			
	150-250μ	90-150μ	60-75µ	20-30μ	150-250μ	90-150μ	60-75µ	20-30µ
Agglutinates	5.3	5.2	6.5	12.5	54.2	60.3	56.5	43.5
Microbreccias								
Recrystallized	57.5	47.2	36.5	15.5	19.2	20.5	16.5	7.0
Vitric	6.9	6.8	16.5	5.5	4.4	3.0	1.0	0.5
Angular Glass Fra	gments							
Brown	2.3	6.2	4.0	7.0	7.2	4.3	8.0	6.5
Colorless	0.3	2.6	1.5	5.0	2.0	3.0	3.0	3.5
Pale Green	0.3	-	-	==	0.2	-	-	-
Glass Droplets								
Brown	0.8	2.0	0.5	2.0	2.2	0.3	2.0	7.0
Colorless	-	0.2	-	-	0.2	0.3	-	
Ropy Glasses	1-1	_	_			1.0	0.5	-
Clinopyroxenes	4.1	8.0	15.5	18.5	3.0	2.3	5.5	18.5
Orthopyroxenes	1.2	2.0	2.5	9.5	1.2	1.3	4.5	5.0
Plagioclase	5.6	6.6	11.5	21.5	3.6	2.3	1.5	7.0
Olivine	0.5	0.4	1.5	0.5	1.0	-	-	-
Opaque Minerals	-	-	-	-		= -1	1	1.5
Basalt	5.9	4.2	0.5	T	0.8	1.3	-	5 3
Anorthosite	0.3	1.2	-	_	0.2	-	_	
Tachylite	8.9	7.0	3.0	2.5	3+4	-	1.0	-
No. of Grains								
counted	400	500	200	200	500	300	200	200

shock modification as a consequence of the impact environment. Many plagioclase crystals have been disrupted by shock to such an extent that they have been converted to diaplectic glasses.

Plagioclase is the ubiquitous mineral in the lunar soils. The anorthite content is generally high in any soil although the range of values in mare soils is generally greater (An_{60} to An_{98}) than in highland soils (generally An_{90} or higher); highland plagioclases, however, may also have a large compositional range (Fig. 6.17) (Apollo Soil Survey, 1974).

A small number of K-feldspar grains have been encountered in the lunar soils. Most are small and attached to, or intergrown with, plagioclase. They generally have an Or range of from 70 to 86 mole per cent.

Pyroxenes are present in most soils and like the plagioclase frequently show signs of shock modification. In mare soils they are almost exclusively clinopyroxene (augite) derived from the mare basalts. Highland soils contain a relatively large proportion (over a third) of orthopyroxene as well as clinopyroxene. The pyroxenes in the highland soils probably were mainly derived from norite and highland basalt clasts in the crystalline breccia basement rock, although pyroxenes are common as mineral clasts in many highland breccias. The orthopyroxenes are mostly bronzites but range from En_{8.5} to En_{6.1}. In Fig. 6.18 detrital pyroxenes from highland soils (Apollo 14) are contrasted with pyroxenes from the mare sites (Apollos 11 and 12). Augites and subcalcic augites dominate the mare pyroxenes whereas the highland pyroxenes extend into the low-calcium range (Apollo Soil Survey, 1974). Mare pyroxenes are also distinguished from their highland equivalents by the presence of extreme compositional zoning.

The pyroxene/plagioclase ratio of most texturally mature soils consistently increases with decreasing grain size (Table 6.7; see sample 14003). This may simply reflect the differing mechanical properties of the two minerals or, as Finkelman (1973) has suggested, it may be due to fine grain sizes being transported over greater distances. However, the net result is an increase in mafic elements in finer grain sizes which has considerable bearing on the chemistry of some glass particles (particularly agglutinates which are discussed in a following section).

Olivine is present in most soils but is very variable in proportion. Only some mare basalts contain a large percentage of olivine so there is a tendency for it to vary from sample to sample at any one mare site. Olivine is generally only present in small amounts (7 per cent) in highland soils, where it is probably derived from pre-existing troctolite fragments and perhaps from a "dunite" source. The olivines mostly lie in range of Fo_{75} to Fo_{60} with a peak around Fo_{67} (Fig. 6.19). A few grains are either extremely magnesian (Fo_{89}) or extremely iron-rich (Fo_{14}) (Apollo Soil Survey, 1974). In general

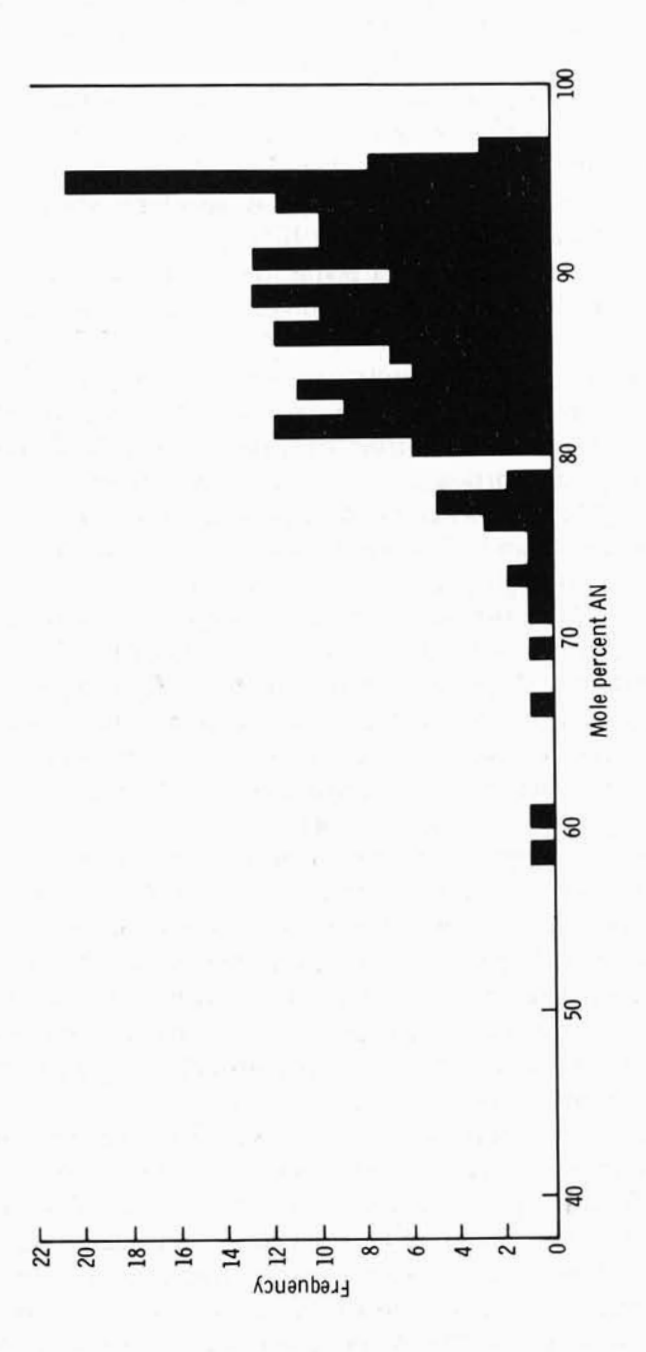


Fig. 6.17. Histogram of plagioclase from highland soils collected by Apollo 14 (from Apollo Soil Survey, 1974).

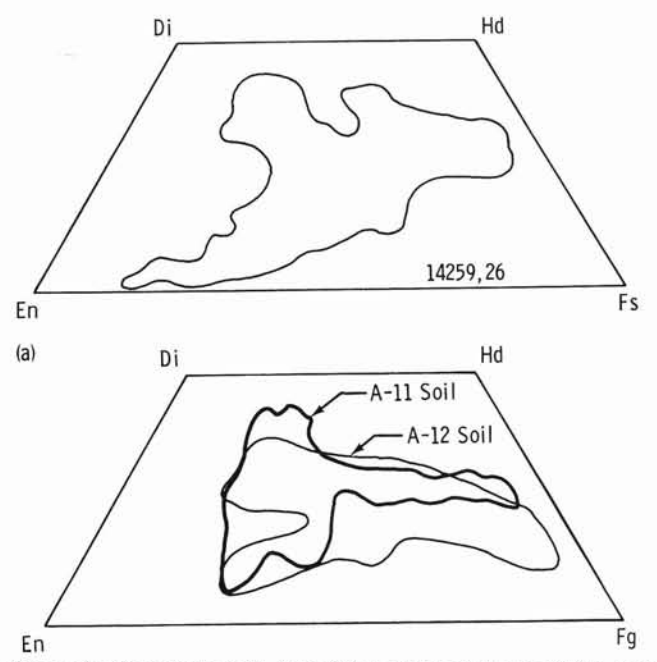


Fig. 6.18. Composition of pyroxenes in soils from (A) a highland site and (B) a mare site. Note the extrusion of the highland pyroxene field towards the low-Ca enstatite apex (after Apollo Soil Survey, 1974).

the compositional range of olivines is larger in highland soils than in mare soils.

Most soils contain some opaque minerals, mainly ilmenite. The ilmenite is probably largely basaltic in origin at both mare and highland sites. It is very variable in amount and can be quite abundant in some mare soils such as the Apollo 11 site where it forms a large percentage of the basement rock. A variety of other minerals such as spinels are present in the soils but in minor amounts only.

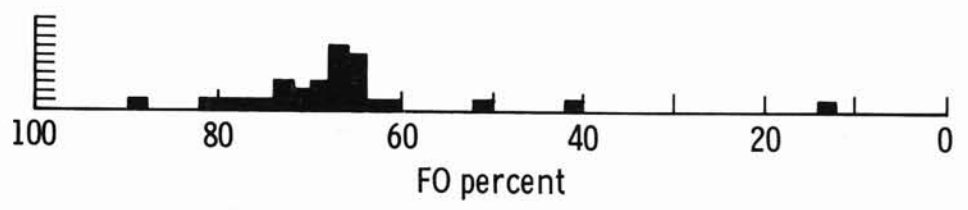


Fig. 6.19. Histogram of olivine compositions in an Apollo 14 soil, expressed as mole per cent forsterite (after Apollo Soil Survey, 1974).

Metallic Particles

Metal grains are present in very small numbers in all of the lunar soils. The particles are generally small, few being larger than 100 μ m, and consist largely of kamacite and taenite and in some cases schreibersite and troilite. Some particles are free standing metal whereas others are associated with a silicate assemblage. Bulk chemistry of the particles indicates that they originate in three ways: (1) Many particles, particularly in mare areas, come from igneous rocks, (2) a proportion, however, are relatively unmodified meteoritic materials whereas (3) others are metallic spheroids which appear to be impact melted fragments of the meteoritic projectile (Goldstein *et al.*, 1972). The composition of the meteoritic materials suggests that they are chondritic in origin (Fig. 6.20).

Glass Particles

Glass particles are abundant in the lunar soils and provide some of the clearest insights into its provenance and to some extent its evolution. Compositionally and morphologically the glasses are extremely complex but they can conveniently be divided into two broad categories: (1) glasses which are essentially homogeneous and (2) agglutinates which are extremely inhomogeneous.

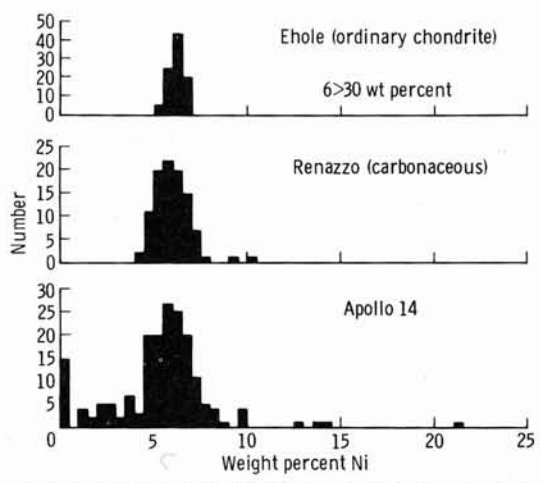


Fig. 6.20. A comparison of nickel distributions in metal fragments from Apollo 14 soils compared to metal separates from chondritic meteorites (after Goldstein et al., 1972; Proc. 3rd Lunar Sci. Conf., Suppl. 3, Vol. 1, MIT/Pergamon).

Homogeneous Glasses

The homogeneous glasses are morphologically diverse. However, most are angular jagged fragments obviously derived from larger glass fragments by comminution. A smaller number of glass particles which caught the attention of many people following the first lunar mission have rotational forms. The particles range from perfect spheres, to oblate and prolate spheroids, to dumbbell (Fig. 21) and teardrop shapes (Fig. 6.22). Some particles have detrital rock or mineral fragments as cores (Fig. 6.22). Others have a small number of mineral fragments dispersed through otherwise homogeneous glass. Some glasses are vesicular with vesicles forming as much as 30 per cent of the particle volume. In the extreme some spheres are actually hollow bubbles which are as large as 2 cm in at least one case (Fig. 6.23).

Variations of the morphology of rotational glass forms may be explained in terms of the surface tension of the molten glass, and the angular velocity of the spinning glass mass as it is ejected from the impact crater. The developmental sequence, from a sphere controlled entirely by surface tension to a dumbbell form as angular velocity increases, is shown in Figure 6.24 (Fulchignoni *et al.*, 1971). Obviously, the survival of a rotational form

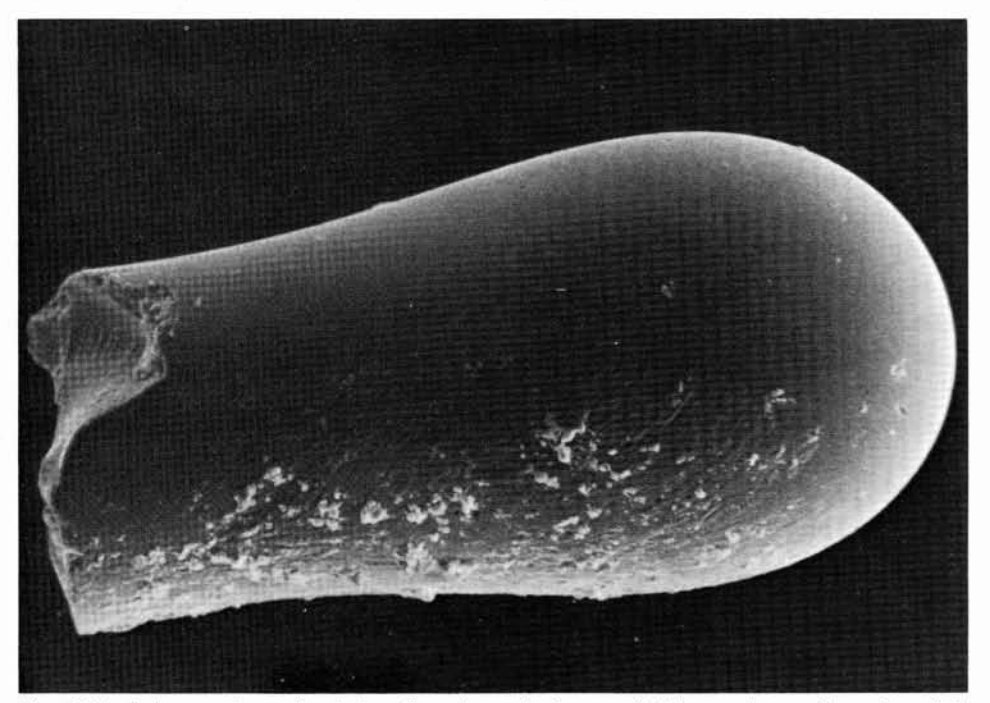


Fig. 6.21. A fractured rotational glass form from the lunar soil. The maximum dimension of the particle is $220\,\mu m$ (NASA Photo S-72-52308).

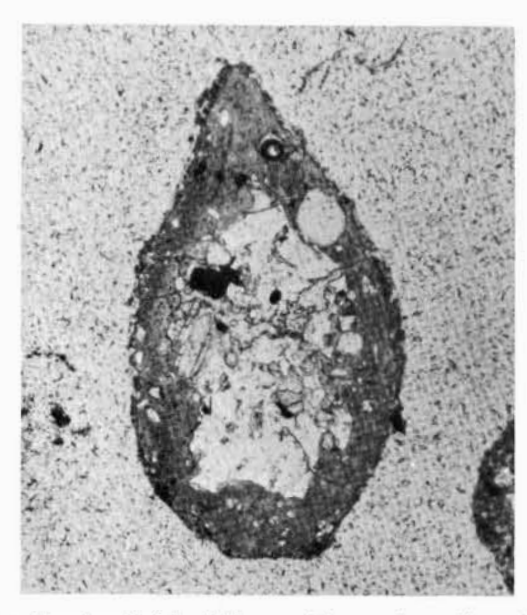


Fig. 6.22. A brown glass "teardrop" with a lithic core. The maximum dimension of the particle is 120 μ m (NASA Photo S-72-46170).

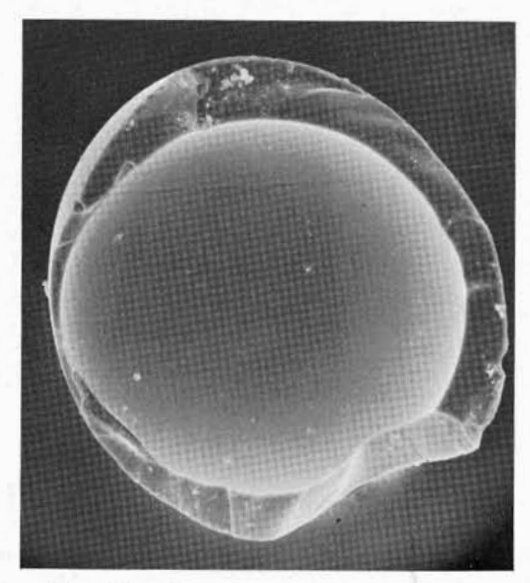


Fig. 6.23. Broken hollow glass sphere from an Apollo 12 soil. Note variation in wall thickness. The particle is approximately 100 μ m is diameter.

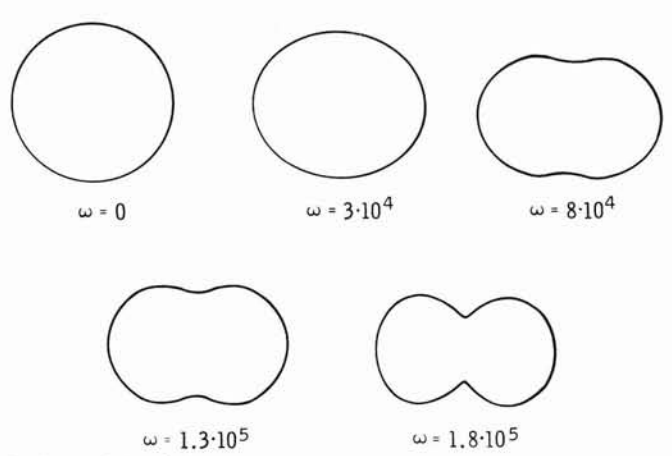


Fig. 6.24. Evolution of the various rotational forms as a function of angular velocity (ω) (after Fulchignoni et al., 1971; Proc. 2nd Lunar Sci. Conf., Suppl. 2, Vol. 1, MIT/Pergamon).

depends upon it having cooled below its transformational temperature before it intersects the lunar surface again. The available time will depend upon event magnitude and trajectory. Englehardt et al. (1973) has found evidence of cooling rates of 100°C s⁻¹ for spherules from the Apollo 15 site, suggesting that relatively small impact events could produce rotational glass forms. From Figure 6.25 it can be seen that spherical and rotational glass forms occur throughout the soil but in a restricted grain-size range. The grain size restriction is probably connected with the cooling rate of the glass during transit and the surface tension of the glass. Larger glass forms simply do not cool fast enough to survive secondary impact with the lunar surface. Spheres and other rotational forms are not abundant in any size range and deserve considerably less attention than they received during the early phases of the Apollo program. However, it is worth comparing the distribution of spheres and rotational forms in the Apollo 16 soils with the Apollo 17 soils (Fig. 6.26). The Apollo 17 soils contain a large volcanic pyroclastic contribution most of which consists of glass spheres (see Chapter 4). Consequently concentrations of spheres and rotational forms of 5 per cent or more are not uncommon at the Apollo 17 site.

Homogeneous glasses come in a wide variety of colors – colorless, white, yellow, green, orange, red, brown and black. Most particles have darker colors such as brown or black. In general terms the darker glasses contain more Fe and Ti whereas the lighter glasses tend to be more aluminous. The refractive index of these glass particles ranges from 1.570 to 1.749 and like the color it varies directly with the total Fe and Ti content and inversely with the Al content (Chao et al., 1970) (Fig. 6.27). The lighter colored glasses with a low refractive index tend to be more anorthositic or

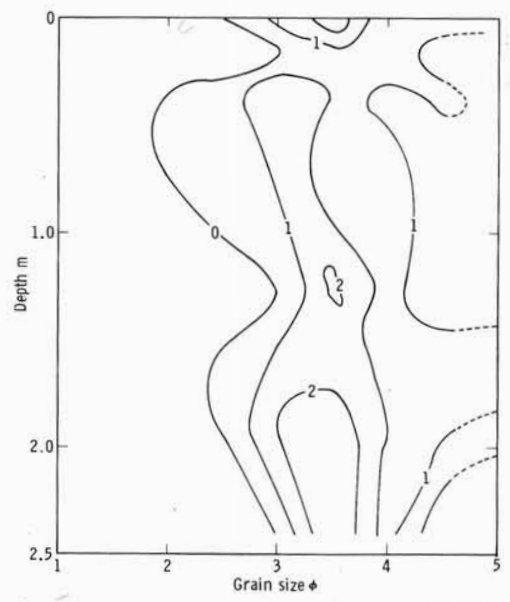


Fig. 6.25. Distribution of rotational glass forms (mainly spheres) as a function of both depth and grain size in the Apollo 16 deep drill core. Spheres tend to concentrate in a size range of from 3 to 4ϕ (125 to 62.5 μ m)which suggests that scaling factors relating to surface tension and cooling rate control their formation. Concentrations are expressed as number per cent per 0.5ϕ grain size interval.

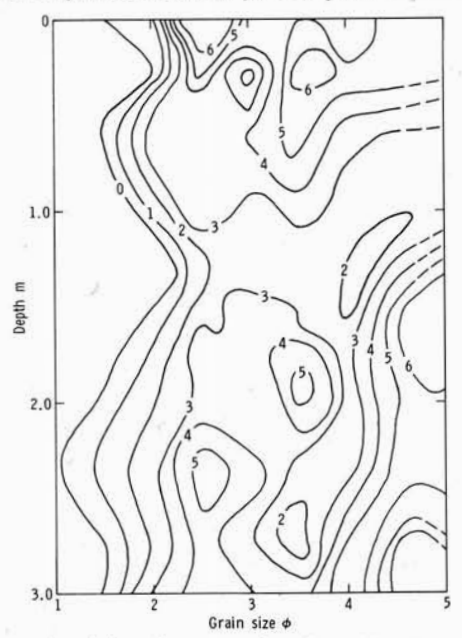


Fig. 6.26. Distribution of rotational glass forms as a function of depth and grain size in the Apollo 17 deep drill core. The higher concentrations of these particles in the Apollo 17 core by comparison with the Apollo 16 core is a concequence of the addition of large volumes of volcanic pyroclastic materials to the soil. Concentrations are expressed as number per cent per 0.5ϕ grain size interval.

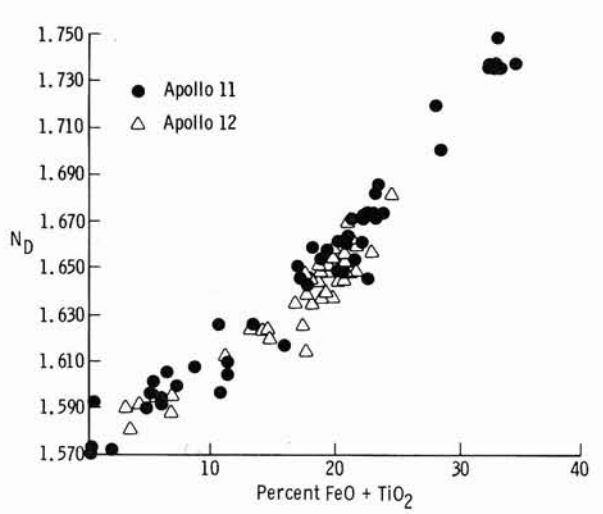


Fig. 6.27. Positive correlation of indices of refraction (N_D) of lunar glasses with the total FeO and TiO₂ content (after Chao, E., Boreman, J., Minkin, J., James, O. and Desborough, G., *Jour. Geophys. Res.*, 75: 7445-7479, 1970; copyrighted American Geophysical Union).

"highland" in composition, whereas the darker glasses with a high refractive index tend to be basaltic or "mare" in composition. The angular and rotational glass forms have the same range of colors and refractive indices, suggesting a common origin.

Chemistry of Homogeneous Glasses

The regular form of many homogeneous glasses suggests that they are impact melts sprayed onto the lunar surface during crater excavation, probably during the jetting phase. Terrestrial analogs indicate that in general the major element chemistry of the bedrock survives unchanged in an impact melt (Fredricksson *et al.*, 1974). Consequently, the homogeneous lunar soil glasses have been studied intensively in order to gain an insight into soil provenance and the composition of the lunar crust (Reid *et al.*, 1972a, 1972b; Reid, 1974; Ridley *et al.*, 1973; Apollo Soil Survey, 1971).

In Tables 6.8 and 6.9 the main compositional glass types are presented for two areas, the Apollo 15 site which is essentially a mare site, and the Apollo 14 site which is situated in the lunar highlands. The Apollo 15 data are particularly instructive in that the site is on the mare surface but a short distance from the Apennine Front. Both highland and mare rock compositions are, therefore, well represented. To add to the complexity of the Apollo 15 site the soils also contain a modest proportion of green-glass particles. These particles are basaltic in composition and are believed to be pyroclastic in origin.

A total of eleven compositional types occur among the homogeneous

TABLE 6.8

Average composition of homogeneous glass particles from the Apollo 15 soils (after Reid et al., 1972b).

			MARE B	ASALT	
	Green Glass	Mare 1	Mare 2	Mare 3	Mare 4
SiO ₂	45.43 (.63)	45.70 (2.01)	44.55 (1.94)	43.95 (1.89)	37.64 (2.27)
TiO ₂	.42 (.06)	1.60 (.43)	3.79 (.98)	2.79 (.93)	12.04 (2.00)
Al ₂ O ₃	7.72 (.33)	13.29 (1.96)	11.77 (1.88)	8.96 (1.20)	8.46 (1.07)
Cr ₂ O ₃	.43 (.03)	.33 (.07)	.26 (.06)	.46 (.11)	.48 (.10)
FeO	19.61 (.84)	15.83 (2.16)	18.83 (2.14)	21.10 (1.46)	19.93 (1.76)
MgO	17.49 (.54)	11.72 (1.60)	8.84 (1.88)	12.30 (1.60)	10.49 (1.58)
CaO	8.34 (.41)	10.41 (.80)	10.46 (.94)	9.02 (.70)	8.81 (1.40)
Na ₂ O	.12 (.05)	.30 (.14)	.34 (.20)	.27 (.12)	.54 (.17)
К2О	.01 (.02)	.10 (.07)	.13(.11)	.05 (.03)	.13 (.05
TOTAL	99.57	99.28	98.97	98.90	98.52
Percentage of total analyses	34.2	12.2	3.8	4.8	1.1

Numbers in parentheses are standard deviations.

glasses from the Apollo 15 site (Table 6.8) (Reid et al., 1972), of which green glass particles are the most common. In terms of its normative composition it is a pyroxenite. Mg and Fe are high, Al, Ti and alkalis are low. The composition is essentially mare basalt with more Mg and Ti. The green glasses are mostly spheres and a few contain olivine needles (Fo₇₄). The origin of this glass has been discussed in Chapter 4. The general consensus at the present time is that they are pyroclastic materials formed in fire fountains during the flooding of the lunar mare. Orange glasses with a similar composition and morphology are present in the soils from the Apollo 17 site. At this site the pyroclastic contribution is 100 per cent of one soil sample, up to 22 per cent of other soil samples and results in anomalously high Zn concentrations (Rhodes et al., 1974). Mixing model studies show considerable variation in the pyroclastic contribution in surface samples (Fig. 6.28). Spheres and rotational pyroclastic glass forms occur vertically through the soil blanket (Fig. 6.26).

The soils from the Apollo 14 site contain a similar range of compositional types, but the relative proportions of the glasses change in such a way that the amount of highland-derived Fra Mauro basalts increases whereas the mare basalts are of less importance.

A large number of mare glasses are present in the Apollo 14 and 15 soils and are characterized by a high Fe and low Al content. These glasses

	FRA	A MAURO BASA			
Highland Basalt	Low K	Moderate K	High K	'Granite' 1	'Granite' 2
44.35 (2.38)	46.56 (1.78)	49.58 (1.43)	53.35 (2.82)	73.13 (1.36)	62.54
.43 (.37)	1.25 (.45)	1.43 (.30)	2.08 (.56)	.50 (.71)	1.18
27.96 (3.67)	18.83 (1.85)	17.60 (1.54)	15.57 (1.65)	12.37 (.87)	15.73
.08 (.04)	.20 (.05)	.17 (.03)	.12 (.06)	.35 (.49)	.03
5.05 (2.28)	9.67 (1.88)	9.52 (1.31)	10.25 (1.09)	3.49 (3.16)	6.67
6.86 (2.92)	11.04 (1.61)	8.94 (1.24)	5.77 (1.61)	.13 (.10)	2.51
15.64 (1.63)	11.60 (.93)	10.79 (.69)	9.57 (.77)	1.27 (.62)	6.86
.19 (.23)	.37 (.14)	.74 (.14)	1.01 (.42)	.64 (.16)	.98
.01 (.03)	.12 (.07)	.47 (.17)	1.11 (.40)	5.97 (.27)	3.20
100.92	99.66	99.24	98.83	97.85	99.70
6.6	15.0	16.5	5.3	.4	.2

resemble the composition of mare basalts and have been divided into four subtypes at the Apollo 15 site. This site is on the mare surface in Palus Putredinus and undoubtably many of the glasses are local in origin. However, Mare Imbrium, Mare Serenitatis and Mare Vaporum are nearby. The Mare 3 component is very similar to large basaltic rock samples returned from the

Average composition of homogeneous glass particles from the Apollo 14 soils (after Apollo Soil Survey, 1974).

* * 1	Mare-type basaltic glass	Fra Mauro basaltic glass	Anorthositic gabbroic glass	Gabbroic anorthositic glass	'Granitic' glass	Low-silica glass
SiO ₂	45.48 (2.64)	48.01 (1.75)	45,23 (1,00)	47.37 (2.52)	71.54 (7.60)	37.97
TiO ₂	2.77 (2.44)	2.02 (.53)	.36 (.20)	.14 (.12)	.39 (.20)	.23
Al ₂ O ₃	10.86 (3.10)	17.12 (1.83)	25.59 (1.08)	31.32 (1.34)	14.15 (4.21)	34.54
FeO	18.14 (2.93)	10.56 (1.37)	5.59 (1.00)	2.98 (1.51)	1.79 (2.16)	1.19
MgO	11.21 (4.25)	8.72 (1.82)	7.84 (1.49)	2.18 (1.38)	.70 (1.04)	5.57
CaO	9.56 (1.42)	10.77 (.86)	14.79 (.91)	14.78 (2.44)	1.97 (1.84)	20.39
Na ₂ O	39 (30)	.71 (.26)	.25 (.27)	.95 (.60)	.93 (.64)	0.00
K ₂ O	.32 (.42)	.55 (.28)	.12 (.25)	.22 (.22)	6,53 (2.44)	0.00
TOTAL	98.73	98.46	99.77	99.94	98.00	99.89

Numbers in parentheses are standard deviations.

TABLE 6.9

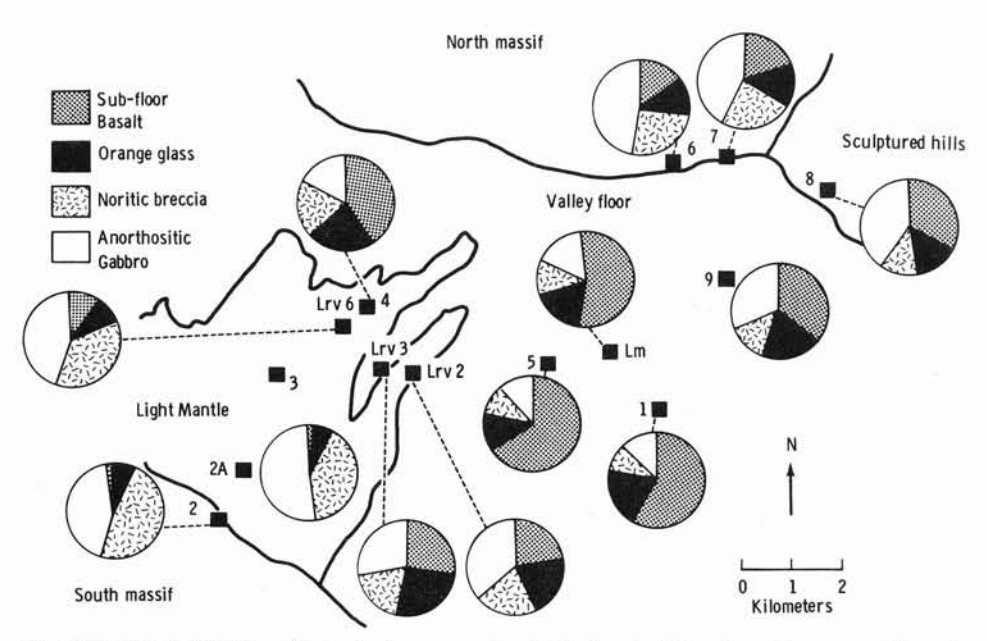


Fig. 6.28. The distribution of pyroclastic orange glass in the Apollo 17 surface soils compared to other local soil components (from Rhodes *et al.*, 1974, *Proc. 5th Lunar Sci. Conf.*, *Suppl. 5*, *Vol. 2*, Pergamon).

site, and is probably of local origin. The other three types can not be directly attributed to particular sources, but Mare 1 glasses are similar to Mare Fecunditatis basalts whereas the Mare 4 glasses are similar to Mare Tranquillitatis basalts. The Mare 2 glasses are most similar to the Mare 3 glasses although there are significant differences such as higher Ca, Al and Sr and lower Fe and Mg content. It is possible that these glasses represent a more feldspathic mare basalt which was not sampled at the Apollo 15 site even though it may have been present.

The Fra Mauro basaltic glasses are a major constituent in the Apollo 15 soils and are comparable to those forming the most abundant glass type in the Apollo 14 soils. They are identical to brown ropy glasses called KREEP (for their higher potassium, rare earth element and phosphorus content) that were originally found in Apollo 12 soils (Meyer *et al.*, 1971) and are analagous to terrestrial tholeiitic basalts. One variant may be from the Apennine Front which is not a typical highland area. This is supported by orbital X-ray fluorescence data which indicates an Al/Si ratio similar to the low-K Fra Mauro basalt (Adler *et al.*, 1972a, 1972b). These glasses are probably representative of the pre-Imbrian crust.

Glasses characterized by a high Al₂O₃ content have been called highland basalt glasses (anorthositic gabbro). This is the anorthositic

component generally held to be characteristic of the highlands. This component is low in the Apollo 15 soils which confirms arguments that the Apennine Front is not typical of the highlands.

Two glass types high in silica have the composition of a potash granite and a granodiorite. They have been found at other sites but are always in minor amounts. Their origin is unknown.

Provenance of Homogeneous Glasses

Reid et al. (1972b) have suggested that the pre-Imbrium surface consisted of Fra Mauro type rocks that had undergone some near surface differentiation. The excavation of the Imbrium Basin resulted in a redistribution of much of the differentiated sequence. The edges of Mare Imbrium were only flooded to a shallow depth by basalt, with the result that craters such as Copernicus, Aristillus and Autolycus penetrated the lava and excavated Fra Mauro material. The Apennine Front provided low-K material, perhaps from greater depths if we assume an inverted ejecta sequence. Apollo 14 sampled the same ejecta blanket but further from the crater rim and hence at shallower depth which accounts for the larger highland-basalt (anorthositic gabbro) content of the Apollo 14 soils. The anorthositic gabbro appears to be the major highland rock type.

The origin of the mare basalts is comparatively well understood and has been discussed in Chapters 1 and 4. Phase relations based on experimental work constrain the basaltic source to a depth of between 100 and 400 km (Ringwood and Essene, 1970; Green et al., 1971). The highland rocks are, however, not so simply explained. It has been concluded from experimental studies that the highland rocks are not partial melts from the same source as the mare basalts (Walker et al., 1973; Hodges and Kushiro, 1973), but that they probably evolved at shallower depths from feldspathic cumulates. The most comprehensive attempt to explain the relationship is that of Walker et al. (1973). They propose that the low-K and medium-K Fra Mauro basalts are derived by partial melting from more feldspathic rocks as outlined in Figure 6.29.

Agglutinates

Agglutinates have also been referred to as glazed aggregates (McKay et al., 1971). or "glass-bonded aggregates" (Duke et al., 1970) but agglutinates are much more complex than these terms suggests (McKay et al., 1971, 1972; Lindsay, 1971, 1972, 1975). They are intimate mixtures of inhomogeneous dark-brown to black glass and mineral grains, many of which are partially vitrified. More than 50 per cent of most agglutinates is

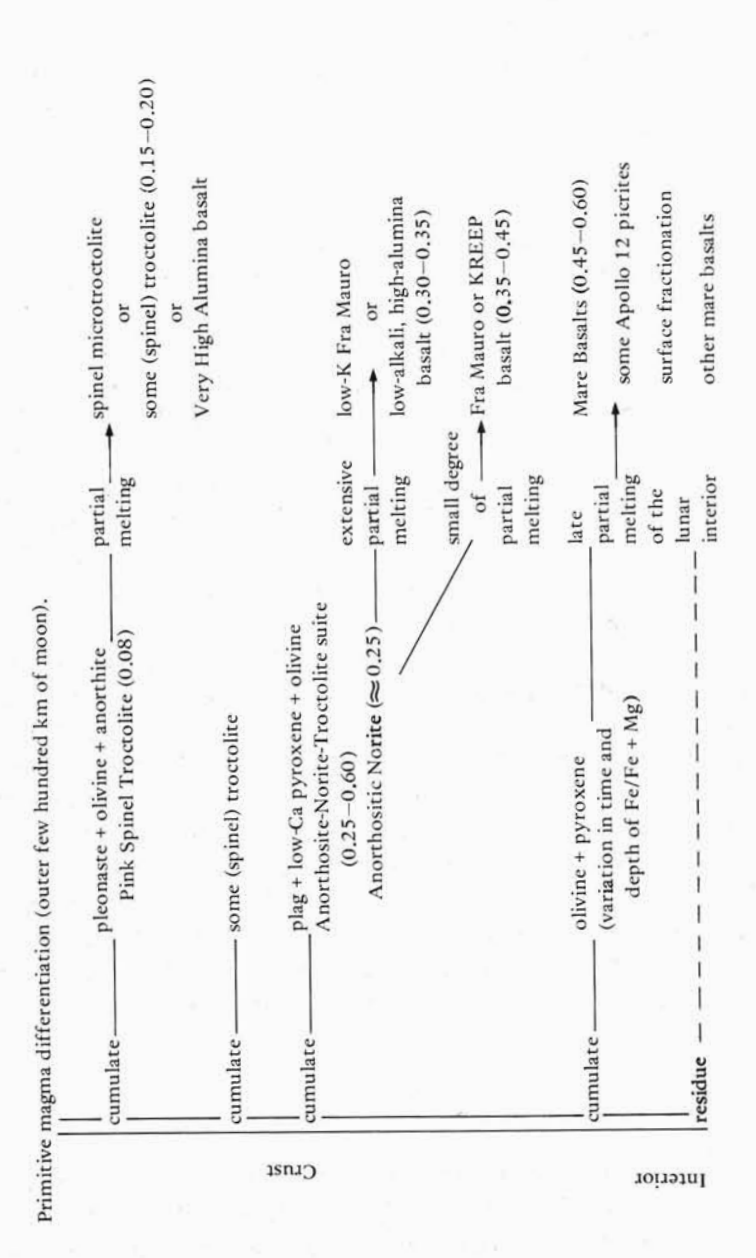


Fig. 6.29. Genetic relationships among highland rocks (from Walker et al., 1973).

mineralic. Most are extremely complex in shape but have a general rounded form suggesting that their final shape was determined by the viscosity and surface tension of the fluid glass (Fig. 6.30). The surface of the grains has a coating of fine detrital fragments which gives them a dull saccaroidal texture (Figs. 6.31, 6.32). Some agglutinates are bowl shaped or take the form of rings or donuts (Fig. 6.31), suggesting that they are "pools" of melt formed in the bottom of microcraters in fine-grained lunar soil (McKay et al., 1972; Lindsay, 1971, 1972c, 1975). Although some consist of dendritic glass projections radiating from a central mineral grain (Fig. 6.33) a few agglutinates are vesicular (particularly larger particles), most are massive and overall less vesicular than the homogeneous glasses.

Chemistry of Agglutinates

The chemical composition of individual agglutinates in a general way reflects the composition of the underlying bedrock. Thus agglutinates from the Apollo 12 site bear a general basaltic imprint (Table 6.10). Because of the inhomogeneity of these glasses more is to be gained from a study of their bulk chemistry than from the chemistry of individual particles. Table 6.11 shows the chemistry of the agglutinate and non-agglutinate fractions of four soils in order of increasing agglutinate content. There are significant differences in chemistry between the two fractions of the soils, and neither fraction is comparable chemically to a major homogeneous glass group (Rhodes *et al.*, 1975). The agglutinate fraction is not constant in composition but varies for a given element roughly in accordance with the bulk soil composition and the agglutinate content; this is particularly so in the case of trace elements. These variations are regular and systematic. That

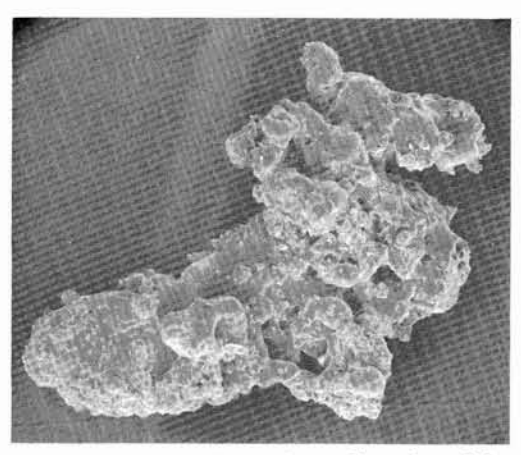


Fig. 6.30. Typical dust coated agglutinate. The maximum dimension of the particle is approximately $180 \mu m$.

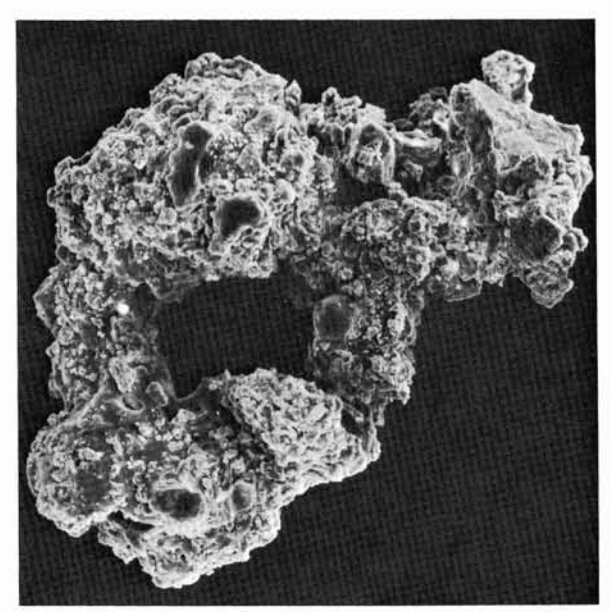


Fig. 6.31. Ring-shaped agglutinate. Such agglutinates support the concept that they are formed by micrometeoroid impact in the lunar soil. The maximum dimension of the particle is approximately 180 μ m.

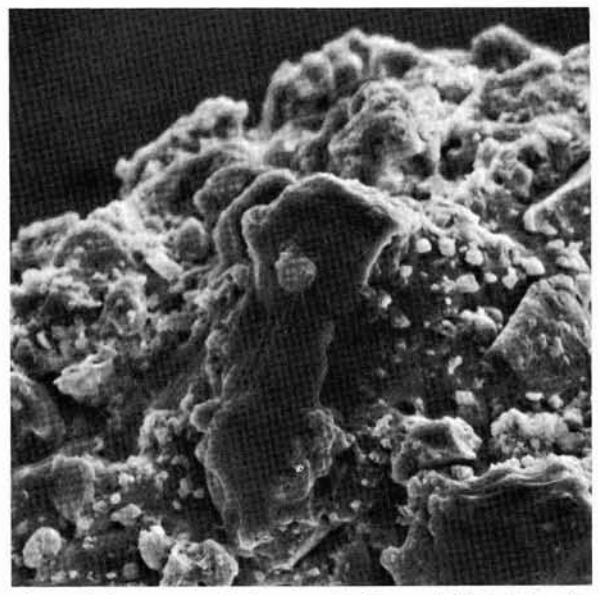


Fig. 6.32. Close-up view of the same agglutinate as in Figure 6.30 showing its dust coated surface Particles of plastically deformed glass adhere to the dust also.

SOIL PETROGRAPHY 265

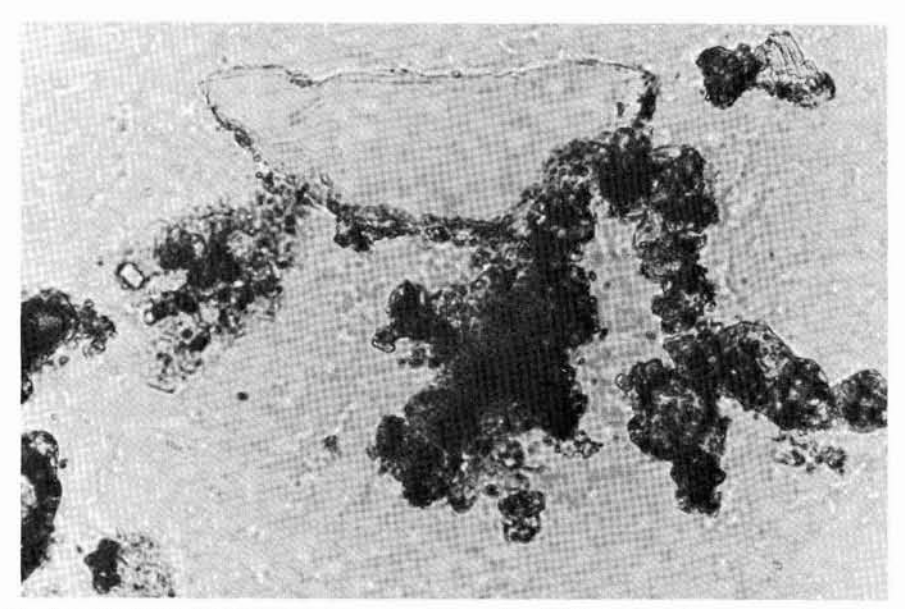


Fig. 6.33. An extremely delicate agglutinate consisting of a detrital mineralic core surrounded by radiating projections of dark-brown glass intimately mixed with fine grained mineralic materials. The maximum dimension of the particle is 230 μ m (NASA Photo S-71-51084).

TABLE 6.10

Chemical analyses of three agglutinates from an Apollo 12 soil (after Chao et al., 1970).

	1	2	3	
SiO ₂	46.7	42.2	44.8	
TiO ₂	2.31	3.34	2.60	
Al_2O_3	15.4	9.8	15.6	
FeO	12.4	18.3	13,7	
MgO	7.9	12.0	7.8	
CaO	10.7	8.9	11.6	
Na ₂ O	0.56	0.32	0.54	
K ₂ O	0.92	0.21	0.23	
P2O5	0.62	0.19	0.17	
MnO	0.10	0.12	0.12	
Cr ₂ O ₅	0.21	0.35	0.29	
NiO		0.04	0.04	
TOTAL	98	96	97	

TABLE 6.11.

Major element chemistry of agglutinate and non-agglutinate fractions of four Apollo 16 soils (after Rhodes et al., 1975).

	65701		61241		61501		64421		
Sample sub samp	March 1967	11	26	26	15	15	18	18	1
fraction wt. fraction	Agglu- tinate	Non-agglu- tinate 0.387	Agglu- tinate 0.571	Non-agglu- tinate 0.429	Agglu- tinate 0.557	Non-agglu- tinate 0,443	Agglu- tinate 0.555	Non-agglu- tinate 0.445	Bulk soil 1.000
Major el	ements (v	vt. %)							
SiO ₂	44.82	45.11	44.99	45.11	44.40	45.09	44.85	44.89	44.97
TiO ₂	0.73	0.52	0.71	0.39	0.69	0.43	0.68	0.43	0.53
Al ₂ O ₃	25.66	27.85	25.41	29.31	25.29	28.40	26.32	29.08	27.82
FeO	6.61	4.57	6.58	3.49	6.57	4.03	6.07	3.77	4.71
MnO	0.09	0.06	0.09	0.05	0.09	0.06	0.08	0.06	0.05
MgO	6.52	5.39	6.68	4.23	6.74	5.13	5.99	4.37	5.36
CaO	14.91	15.85	14.85	16.57	14.72	16.11	15.22	16.45	15.71
Na ₂ O	0.39	0.50	0.50	0.54	0.48	0.53	0.46	0.48	0.58
K20	0.15	0.12	0.12	0.09	0.13	0.10	0.12	0.09	0.11
P2O5	0.11	0.15	0.12	0.07	0.11	0.11	0.13	0.09	0.09
S	0.08	0.05	0.07	0.03	0.08	0.03	0.08	0.03	0.05
Total	100.07	100.17	100.12	99.88	99.30	100.02	100.00	99.74	99.98

is, there appears to be some form of chemical fractionation associated with agglutinate formation. In all cases the agglutinates are enriched in all of the ferromagnesian elements (Fe, Ti, Mg, Mn, Cr, Sc) and most of the lithophile elements (K, La, Ce, Sm, Yb, Lu, Hf, Th, Ta) and depleted in those elements which are characteristic of plagioclase (Al, Ca, Na, Eu). The agglutinates seem to be enriched in elements that igneous systems tend to concentrate either in mesotasis material or mafic minerals, especially clinopyroxene, but are excluded by plagioclase (Rhodes et al., 1975). Rhodes et al. (1975) have suggested that the chemical differences result from selective melting and assimilation of mesostasis material and mafic soil components, such as pyroxene and ilmenite, into the agglutinate glass by a multistage fluxing process. However, in light of the fact that the pyroxene/plagioclase ratio increases in finer fractions of the soil and the fact that agglutinates preferentially incorporate materials finer than 2.5ϕ (177 µm), it appears more likely that the chemical differences relate either to the different mechanical properties of the mineral components, or to selective sorting of the mineral components during transport and deposition.

It thus seems most likely that agglutinates are formed by shock melting and partial melting of fine-grained detrital materials by micrometeoroid SOIL PETROGRAPHY 267

impact (McKay et al., 1972). Their morphology tends to suggest that an impact produces only one agglutinate. This observation has been used to obtain information about the ancient meteoroid flux (Lindsay and Srnka, 1975). As is discussed in more detail in a following section, an impacting meteoroid fuses about five times its own mass of target material with the result that the size distribution of agglutinates tends to be controlled by the mass frequency distribution of micrometeoroids. The longer a soil is exposed to the micrometeoroid flux the higher the content of agglutinates. The agglutinate content can be directly related to the exposure age of the soil as determined from fossil cosmic ray tracks (Fig. 6.34) (McKay et al., 1972; Arrhenius et al., 1971).

Grain Size of Agglutinates

Agglutinates are constructional particles and contain an abundance of fine-grained detrital materials. The included particles are generally finer than 3ϕ (125 μ m) and have a median size of close to 4.7 ϕ (38 μ m) (Lindsay, 1972c). The median grain size of included detritus varies from particle to particle depending upon the size of the agglutinate. The included particles are poorly sorted and have distributions similar to the fine tail of the bulk soil. An agglutinate thus removes finer detrital materials from circulation by incorporating them into a larger complex particle.

Single agglutinates may be as large as 0ϕ (1 mm), although rarely, and comminuted agglutinate fragments occur in abundance in particle sizes as small as 6ϕ (16 μ m). However, most unbroken agglutinates occur in a narrow size range between about 2ϕ (250 μ m) and 2.5 ϕ (178 μ m) (Fig. 6.35). As

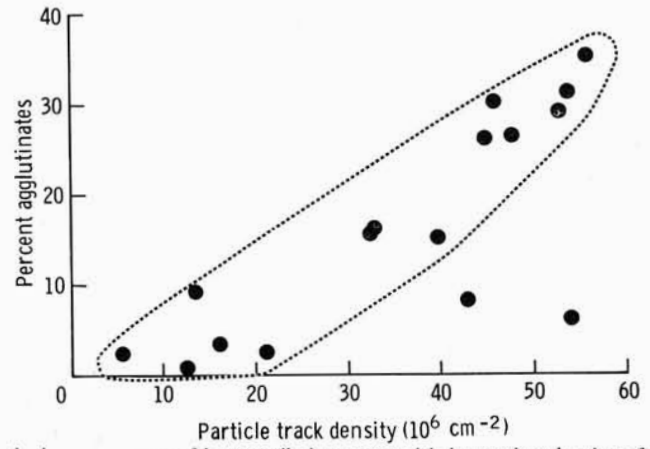


Fig 6.34. The agglutinate content of lunar soils increases with increasing density of fossil cosmic ray particle tracks, suggesting that exposure time at the lunar surface determines agglutinate content (adapted from McKay et al., 1972; Proc. 3rd Lunar Sci. Conf., Suppl. 3, Vol. 1, MIT/Pergamon).

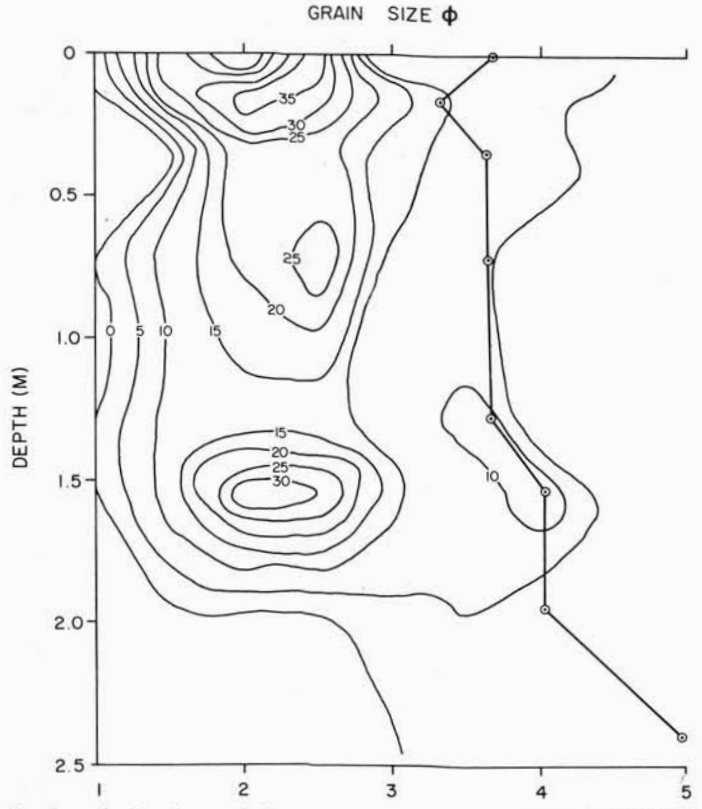


Fig. 6.35. Distribution of unbroken agglutinates as a function of grain size and depth in Apollo 16 drill core samples. Concentrations are expressed as number per cent per 0.5ϕ grain size interval. Most agglutinates are concentrated at a grain size of 2.5ϕ (177 μ m) (from Lindsay, 1975).

discussed previously, the proportion of agglutinates in any one sample varies considerably apparently as a function of exposure age (McKay et al., 1972). Agglutinate concentrations fluctuate, therefore, with depth (Fig. 6.35). Typically the size distribution of unbroken agglutinates has a mean of 2.45ϕ (184 μ m) and is moderately to moderately-well sorted ($\delta_{\rm I}=0.80\phi$). The distribution is generally fine skewed (Sk_I = 0.189) the coarse end of the distribution apparently being truncated. The kurtosis of the distribution approaches log-normal at 0.924. Agglutination thus removes the fine end of the bulk soil grain-size distribution and shifts it to the coarse side of the mean grain size of the bulk soil.

The grain-size distribution of the agglutinates appears to be controlled by a complex of variables, but to a large extent it is a direct function of the meteoroid mass-frequency distribution. At the root-mean-square velocity of 20 km s⁻¹ a meteoroid fuses or vaporizes about 7.5 times its own mass of detrital materials (Gault *et al.*, 1972; Lindsay, 1975). Assuming that the

detrital material enclosed in the agglutinate forms part of the solid-liquidmixture transition, an agglutinate should be about 5 times the mass of the impacting meteoroid. The size distribution of agglutinates on the fine side of 2.2ϕ (217 µm) fits the model well. However, on the coarse side of 2.2ϕ the size distribution is depleted by comparison with the micrometeoroid flux. This implies that agglutination is inhibited by a second variable, which relates to scale (Lindsay, 1975). The most likely variables are viscosity and surface tension of the melt. Agglutinate formation relies on the ability of the melt to maintain its integrity during crater excavation. As event magnitude increases the probability that an agglutinate will form decreases, because the glass is dissipated as small droplets. Consequently the agglutinate grain-size distribution is fine skewed and by comparison with the meteoroid flux it is excessively deficient in coarser particles. The standard deviation of the agglutinate distribution cannot, therefore, be larger than the standard deviation of the meteoroid flux; it is in fact about half of the equivalent flux value.

The mean agglutinate size distribution suggests that most agglutinates are formed by micrometeoroids in the mass range 5.5×10^{-5} to 7.0×10^{-8} g. This mass range includes approximately 68 per cent of the mass and hence of the kinetic energy of the meteoroid flux. Obviously, agglutinate formation is one of the major processes active in the reworking of mature lunar soils.

The Genetic Environment of Agglutinates

Agglutinates are the product of extreme shock induced pressures of very short duration. Experimental data suggest that shock-produced melts are not formed in significant amounts in the lunar soil at pressures below 100 kbar (Gibbons et al., 1975). At 250 kbar only 1 to 2 per cent of melt is formed, and some of the plagioclase is transformed to maskelynite. Plagioclase is completely transformed to maskelynite at 288 kbar and about 5 per cent of the mass is shock-vitrified. The melt content increases to approximately 20 per cent at 381 kbar. When pressures are elevated to 514 kbar there is approximately 50 per cent glass and virtually all plagioclase is melted. The intergranular melt is vesicular and there are prominent schlieren (Gibbons et al., 1975). The experimental work suggests that most natural agglutinates are probably formed at shock induced pressures of between 381 kbar and 514 kbar.

Mixing Models and End Members

It is readily apparent from the homogeneous glass compositions that

the lunar soil is a complex mixture of several major lithologies (Chao et al., 1970; Apollo Soil Survey, 1971; Reid et al., 1972, 1973; Lindsay, 1971). However, by themselves the glasses do not give us more than a general feeling for the relative importance of the various components or end members, nor do they offer complete information concerning variations in the mixture at a particular locality. This problem can be approached directly through mixing models. A general mixing model for N end members can be defined as:

$$O_{i} = \sum_{j=1}^{N} a_{j} X_{ij} + e_{i}$$
 (6.3)

where O_i is the observed percentage of the i^{th} oxide (or element) in the bulk soil, a_j is the proportion of the j^{th} end member contained in the soil, X_{ij} is the percentage of the i^{th} oxide (or element) in the j^{th} end member and e_i is the random error term associated with the i^{th} oxide or element. End-member proportions can thus be estimated by a least-squares solution and the fit of the model can be assessed from the percentage of total corrected sums of squares accounted for.

Several attempts have been made to estimate end-member proportions using models similar to equation 6.3. The basic problem in this approach is the determination of meaningful end member compositions. Some authors have proposed as few as two end members (Hubbard et al., 1971), a mare basalt and a Fra Mauro basalt (KREEP) end member; others have proposed as many as five or six end members (Goles et al., 1971; Meyer et al., 1971; Schonfeld and Meyer, 1972). These end members have been proposed largely on intuitive reasoning and some have little statistical significance. Lindsay (1971) attempted in essence to reverse the mixing model calculations by using factor analysis to separate statistically meaningful endmember groups from chemical analyses of glass. This led to the recognition of three end members (1) an average mare basalt, (2) an average anorthosite, (3) an average Fra Mauro basalt (KREEP). These end members agree well with the Reid et al. (1972b) model for the provenance of homogeneous glasses. One end member represents the mare basalt composition, one the typical anorthositic crustal material and the third the deeper materials excavated by the Imbrian event. The results of mixing-model calculations in Fig. 6 show that the Apollo 12 mare soils are dominated by the mare basalt and member, but all have varying proportions of the other two end members. Hubbard et al. (1971) believed the Fra Mauro basalt (KREEP) component of the Apollo 12 soils to be ejecta from Copernicus. The fact that soil 12033 in Fig. 6.36 consists entirely of local mare basalt material

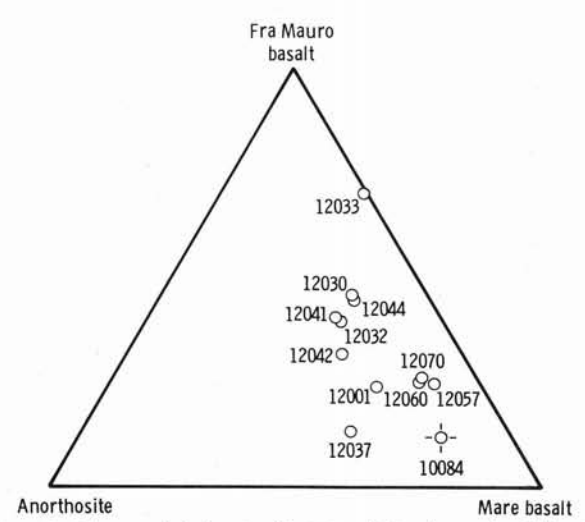


Fig. 6.36. Ternary plot of mixing models for Apollo 11 and 12 soil samples (after Lindsay, 1971).

and Fra Mauro basalt tends to support this suggestion, and emphasize the complex crustal model proposed by Reid et al. (1972b), which suggests that the Fra Mauro component was excavated from beneath a thin mare basalt layer and distributed widely on the lunar surface.

Texture of the Lunar Soil

Grain Size of Lunar Soils

Typically the lunar soils are fine grained and poorly sorted. They are moderately coarse skewed and near log normal in terms of kurtosis. There is, however, a considerable variability in the grain size parameters of samples from any one site (Duke *et al.*, 1970; Lindsay, 1971, 1972c, 1973, 1974, 1975; McKay *et al.*, 1972, 1974; Heiken *et al.*, 1973; Butler and King, 1974; Butler *et al.*, 1973; King *et al.*, 1971, 1972).

The mean grain size of the soils ranges from a coarse extreme of -1.4 ϕ (380 μ m) for a single sample at the Apollo 12 site to an extremely fine grained sample with a mean of 4.969 ϕ (32 μ m) at the Apollo 16 site. The former is believed to be primary detrital material excavated from the bedrock beneath the soil whereas the latter appears to be the product of gaseous sorting, perhaps in a base surge. However, most soils have means close to 4ϕ (Fig. 6.37). For example, the grand mean grain size of 50 samples from the Apollo 15 site is 4.019 \pm 0.334 ϕ (62 μ m) (Lindsay, 1973). Variations in mean grain-size are not random but form part of a time

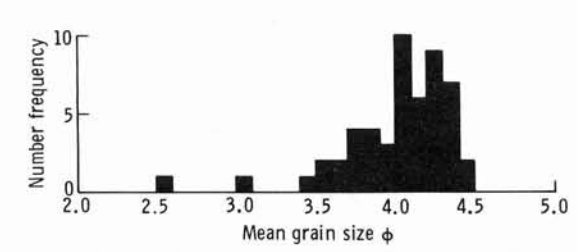


Fig. 6.37. Frequency distribution of the graphic-mean grain size of Apollo 15 core samples (after Lindsay, 1973; Proc. 4th Lunar Sci. Conf., Suppl. 4, Vol. 1, Pergamon).

sequence relating to the amount of reworking each soil layer has undergone. In Figure 6.38 the soil parameters are plotted in stratigraphic context and it can be seen that the mean grain size of the soil decreases upwards in a regular manner, with minor erratic excursions which are probably due to the introduction of either older coarse soils or freshly excavated bedrock material (Lindsay, 1973). Further, the mean grain size of the soil is strongly related to the content of agglutinates on the coarse side of the mean (Fig. 6.39) (McKay et al., 1974). As the soil blanket evolves the accumulation rate decreases and the soil is subjected to longer periods of reworking by micrometeoroids resulting in an increased agglutinate content and a finer mean grain size. It is also apparent from Figure 6.39 that the scatter about the regression line increases as the grain size of the soil decreases. This scatter probably relates to random destruction of large numbers of agglutinates by larger layer forming impact events. More data concerning this process is available from studies of skewness.

The standard deviation or sorting of the lunar soils likewise varies but tends toward values close to 1.8ϕ . The most poorly sorted soils are mixed soils from around Cone Crater at the Apollo 14 site, which have standard deviations in excess of 4ϕ . The most fine-grained soil from the Apollo 16 site is also the most well sorted with a standard deviation of 0.990ϕ . Like the mean, the standard deviation conforms to a time sequence in which the soil becomes better sorted with time (Fig. 6.38) (Lindsay, 1973). Further there is a strong linear relationship between mean and standard deviation which shows that finer soils are better sorted (Fig. 6.40) (Lindsay, 1971, 1972, 1973, 1974; McKay et al., 1974; Heiken et al., 1973). Similarly the better sorted soils contain a greater abundance of agglutinates on the coarse side of the mean.

To this point the relationships are relatively straight forward; with increasing time soils become finer grained, better sorted and show evidence of increased reworking in the form of agglutinates. However, when we attempt to place skewness in the same context the picture becomes more complex. Skewness does not relate in a simple linear way to mean and

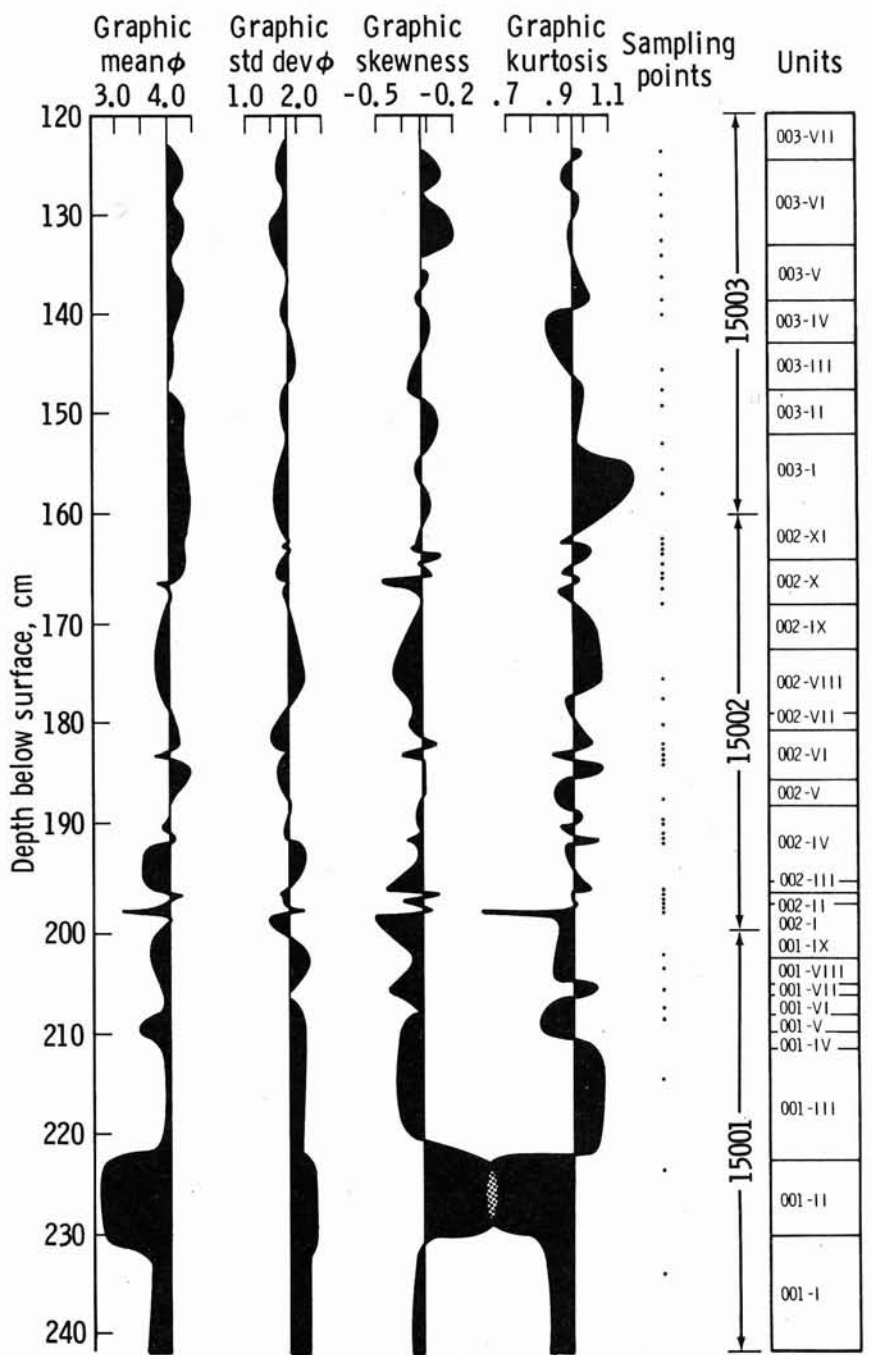


Fig. 6.38. Grain-size parameters for Apollo 15 deep-core samples as a function of depth below the lunar surface. Black areas indicate deviations about mean values (after Lindsay, 1973; Proc. 4th Lunar Sci. Conf., Suppl. 4, Vol. 1, Pergamon).

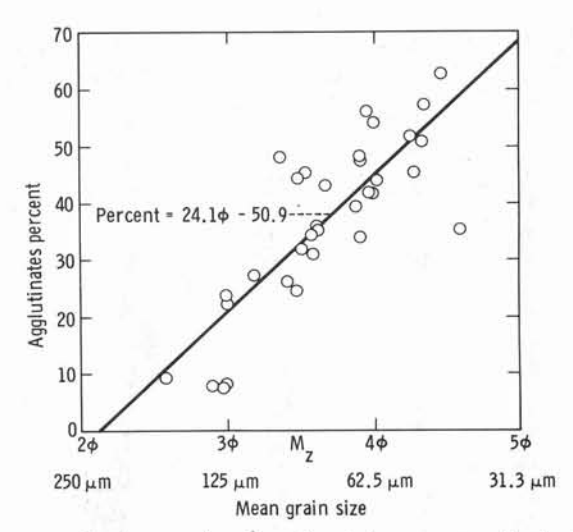


Fig. 6.39. Graphic mean grain size as a function of agglutinate content in the 3.5ϕ to 2.7ϕ (90-150 μ m) fraction of the lunar soil (from McKay et al., 1974; Proc. 5th Lunar Sci. Conf., Suppl. 5, Vol. 1, Pergamon).

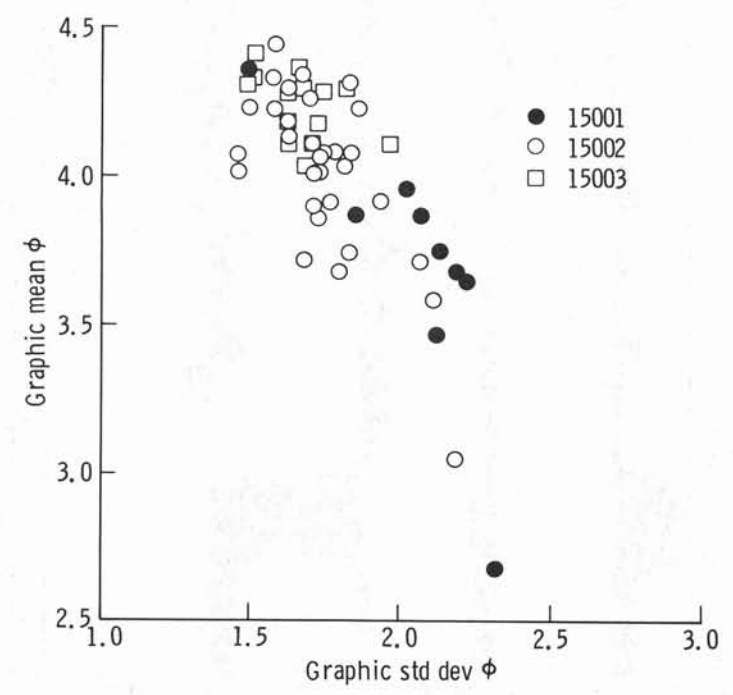


Fig. 6.40. Mean grain size as a function of standard deviation for soils from the Apollo 15 deep drill core (data from Lindsay, 1973).

standard deviation but is controlled by a double function (Fig. 6.41). The formation of agglutinates on the coarse side of the mean could be expected to produce soils that gradually become more negatively (coarse) skewed as the mean and standard deviation become smaller. This relationship does exist but is relatively weak (Fig. 6.38). The second function suggests that a second set of variables is operating to determine the skewness of many soils. The process involved has been called "cycling" (Lindsay, 1975).

Agglutinates are extremely delicate, fragile particles that can be destroyed by comminution much more readily than rock or mineral fragments of equivalent size. The relationship between agglutinate content and exposure age indicates that under normal conditions micrometeoroid reworking produces more agglutinates than it destroys by comminution (Lindsay, 1972, 1975; McKay et al., 1974). This implies that the second function controlling skewness must be due to the destruction of large numbers of agglutinates possibly by larger layer-forming impact events (Lindsay, 1975). The destruction of agglutinates reduces the mean grain-size of the soil and makes the grain-size distribution more symmetrical (i.e. less negatively skewed). The larger the agglutinate content of the soil the more dramatic the effect. Once excavated to the surface micrometeoroid reworking again takes effect and the grain size parameters begin to converge on the ideal evolutionary path. Cycling is thus a series of random excursions during which agglutinates are first formed at the expense of the fine tail of the grain size distribution by micrometeoroid reworking, and are then instantaneously crushed and shifted back to the fine tail again.

Kurtosis appears unrelated to all other grain size parameters and there is no stratigraphic trend to suggest any evolutionary sequence as is seen in the mean and standard deviation (Fig. 6.38). For a log-normal grain-size distribution the kurtosis is 1.0 and most lunar soils fall close to this value. Some soils, however, have kurtosis values of less than 1.0 indicating that the size distribution is excessively broad compared to a log-normal curve. These soils appear to be mixtures in which two or more soils with different grain-size parameters have been brought together to form a broad bimodal or polymodal distribution. Thus, in Figure 6.38 the random deviations in the kurtosis values indicate the introduction of either more primitive soils from deeper in the soil blanket, or freshly excavated bedrock materials (Lindsay, 1975).

Shape of Soil Particles

The shape of soil particles varies considerably, from the smooth spherical form of glass droplets to the extremely irregular and complex

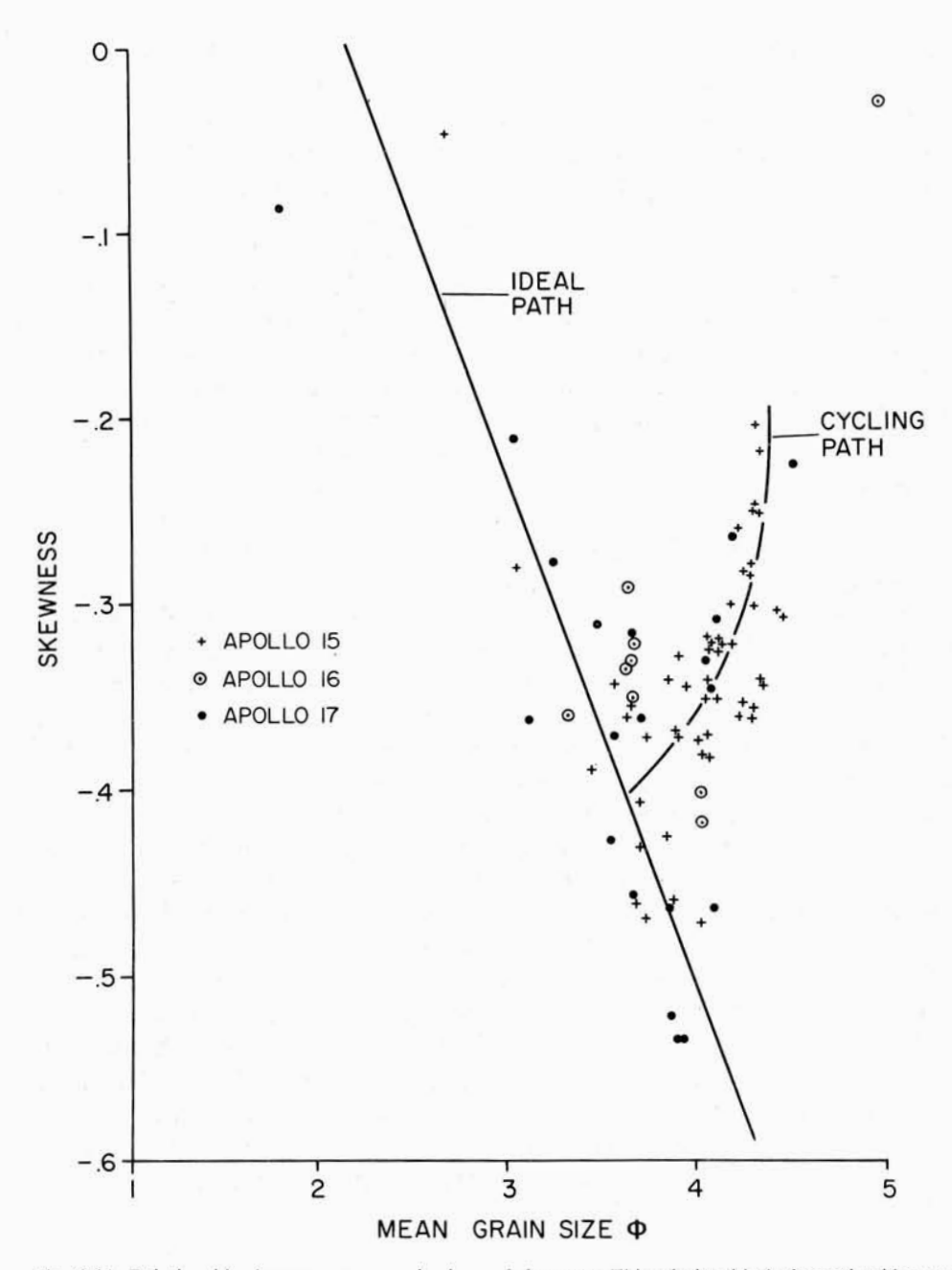


Fig. 6.41. Relationships between mean grain-size and skewness. This relationship is determined by two functions, one an ideal evolutionary path resulting from the gradual addition of agglutinates, the other due to cycling as agglutinates are alternately crushed by larger events and then restored by micrometeoroid reworking at the lunar surface, bringing the skewness back to the ideal path (from Lindsay, 1975).

shapes of agglutinates. Between these two extremes are the blocky angular comminuted rock, mineral and glass fragments. The overall mean sphericity of the soil particles is 0.78 (a value of 1.0 being a perfect sphere). However, perhaps predictably the sphericity of particles varies markedly with grain size and depth in the lunar soil (Lindsay, 1972c, 1974, 1975).

If we look at the sphericity of detrital particles forming a primitive soil (consisting largely of comminuted rock and mineral fragments) we find that sphericity changes in a regular linear manner with grain size. Smaller particles become increasingly more spherical. If we then investigate a texturally mature soil we find that a sinusoidal distribution is superimposed on the general linear trend. Two zones of depressed sphericity develop; one at between 0ϕ (1 mm) and 3ϕ (125 μ m), the other at between 5ϕ (31 μ m) and 7ϕ (8 μ m). The midpoint of these two zones lies close to one standard deviation either side of the mean grain-size of the bulk soil. This relationship is seen to best advantage in Figure 6.42 where sphericity is shown as a function of both grain size and depth in the soil. The zones of reduced sphericity coincide with whole agglutinates on the one hand and comminuted agglutinates on the other. The relationship between particle shape and size thus relates entirely to the textural evolution of the soil and in particular to micrometeoroid reworking at the lunar surface.

Textural Evolution of the Lunar Soil

The texture of the lunar soil evolves in a regular manner in a direct response to continued reworking by the meteoroid flux (Lindsay, 1971, 1972c, 1973, 1975; McKay et al., 1974; Heiken et al., 1973; Butler and King, 1974). The two main dynamic processes responsible for this developmental sequence are (1) comminution and (2) agglutination. The textural maturity of the lunar soil is determined almost entirely by the balance between these two opposing processes, one destructive the other constructive. As a result of this complex interaction between the soil and the meteoroid flux the soil passes through three transitional evolutionary stages (Lindsay, 1975). For convenience the stages are designated (1) the comminution dominated stage (2) the agglutination dominated stage and (3) the steady state or cycling stage (Fig. 6.43).

The Comminution Dominated Stage

Because of the extreme age of the lunar surface few soils have survived that could be assigned to this evolutionary stage. Energetic impact events

striking lunar bedrock produce coarse grained and poorly sorted ejecta. When such loose particulate materials are subjected to repetitive fracture the grain size distribution is gradually modified in such a way that it asymptotically approaches a log-normal form (Kolmogoroff, 1941; Halmos, 1944; Epstein, 1947). The mean grain-size of the particulate materials is

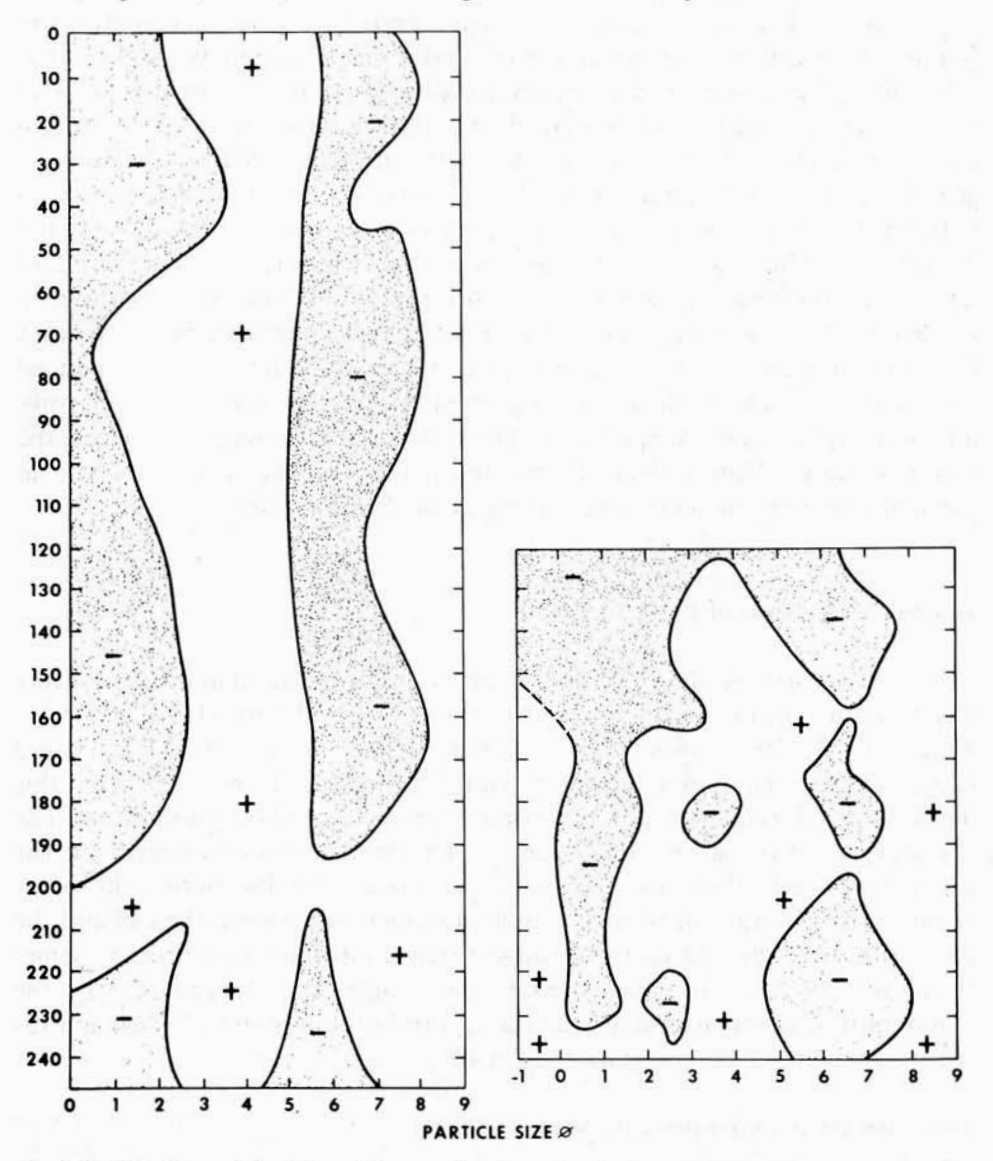


Fig 6.42. Sphericity of detrital particles as a function of grain size and depth in the lunar soil at the Apollo 16 site (left) and the Apollo 15 site (right). Sphericity is expressed as a deviation about the overall mean value of 0.78. Stippled areas are zones of reduced sphericity (from Lindsay, 1975).

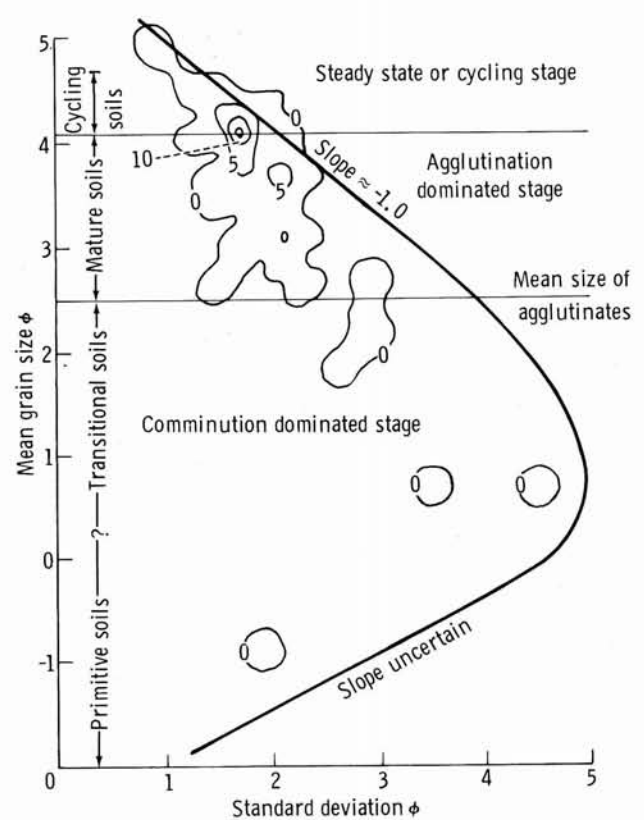


Fig. 6.43. Stages in the evolution of lunar soil as shown by change in mean and sorting of grain-size data. The solid line indicates the evolutionary path for an idealized soil. Contours show density in per cent of soil samples per 0.5ϕ square. Note that most soils are finer than the mean agglutinate size and they concentrate at a mean of 4.1ϕ , the stable point between the two glass modes (after Lindsay, 1974, 1975).

gradually reduced and they become more poorly sorted. These primitive soils are coarse grained with means in excess of 0ϕ (1 mm). During this stage of soil development comminution is the only effective process as most meteoroids interact with single detrital particles. The particles of soil are so large that most micrometeoroid impacts are either involved in catastrophic rupture of grains or they simply form pits on the larger grains.

Experimental studies suggest that cratering occurs in loose particulate material only when the particle mass is less than an order of magnitude larger than the impacting projectile. Thus comminution will dominate soil dynamics until the soil particles are reduced to masses of the order of 10^{-5} g, that is an order of magnitude larger than the mean mass of the meteoroid flux (10^{-6} g). This suggests that the soils would have a mean grain-size of the order of 3.4ϕ ($93~\mu m$). At the very least it is unlikely that agglutination can

become effective until the mean grain-size of the soil is less than 2.5ϕ , the mean grain-size of the agglutinate distribution.

The Agglutination Dominated Stage

Most of the soils presently at the lunar surface appear to be passing through this stage of development. Once the mean grain-size of the soil is small enough for agglutination to be effective, it begins to balance the effects of communition (Duke, 1970; Lindsay, 1971, 1972, 1974, 1975; McKay et al., 1974). This results in a continuing decrease in the mean grain-size as larger lithic and mineral grains are comminuted; the standard deviation of the grain size distribution is reduced causing the ideal evolutionary path in Figure 6.43 to reverse its slope. During this stage there is a strong correlation between mean grain size and standard deviation, and skewness tends to become more negative (Lindsay, 1971, 1972, 1975; McKay et al., 1974; Heiken et al., 1973). The glass particles produced by the two opposing processes (agglutination and comminution) are formed in two narrow size-ranges. Agglutinates concentrate at approximately 2.5ϕ while comminuted agglutinates accumulate at approximately 6ϕ . The distribution of these irregularly shaped particles is clearly shown in Figure 6.42. The mean grain-size of most lunar soils lies between these two glass modes (Lindsay, 1972). Ultimately, as the coarse rock and mineral fragments are broken down by comminution, the mean grain size is forced to lie between the two glass modes at close to 4ϕ and the standard deviation of the soils is restricted to about 1.7ϕ , or roughly coincident with the glass modes. At this point the soils are approaching a steady state. However, agglutination still dominates in that more agglutinates are formed than are destroyed by comminution.

The Steady State Stage

As the evolving soil moves closer to the point of stabilization, where the mean lies between the glass modes, the grain size parameters become more and more dependent on the presence of the agglutinate mode.

At this point a soil may enter a cycling mode. Agglutinates are fragile and readily crushed so that when a soil is redistributed by a larger layer-forming impact event a large proportion of the agglutinate population is destroyed. Removal of the agglutinates causes the mean and standard deviation to decrease and the skewness to become less negative. That is, the soil tends to take on the grain-size parameters of the second glass-mode. The soil is then exposed at the lunar surface to the micrometeoroid flux and agglutination once again become effective, pulling the grain size parameters

back to the steady state ideal. Soils at this stage have been called steady state soils (Lindsay, 1975) or equilibrium soils (McKay et al., 1974).

This model represents an ideal situation where processes are assumed to be operating in a closed system. In reality the soils are continually reworked and soils from two or more stages are continually being mixed. Soils from earlier erosional episodes may be fossilized by burial and later reexcavated to mix with more mature soils at the lunar surface (Lindsay, 1974, 1975; McKay et al., 1975). At the same time larger impact events may penetrate the soil blanket and excavate bedrock material. The result is a complex interbedded sequence of mixed soils which gradually converge to a steady state upward through the stratigraphy (Fig. 6.44). The effects of mixing are well illustrated by the random deviations of kurtosis in Figure 6.38.

Soil Maturity

The term "maturity", when applied to detrital material, is generally used in the sense of a measure of progress along some predetermined path. If we consider sand accumulating on a beach we see several processes operative in modifying the texture and composition of the detrital materials. Wave action abrades, rounds and sorts the detrital particles while less stable minerals deteriorate in the aqueous environment and are removed. The end product is a well-sorted sand consisting of well-rounded quartz grains. In the case of beach sand the proportions of detrital quartz can be used as a measure of maturity. Thus in Pettijohns (1957) concept of maturity monomineralic quartz sand is "the ultimate end product" to which beach

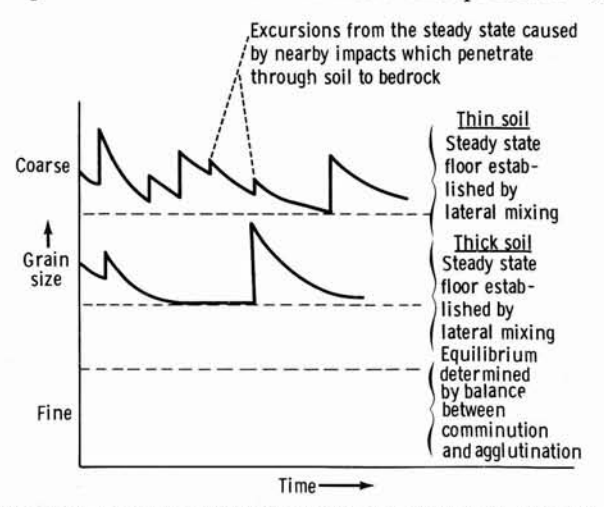


Fig. 6.44. Diagramatic representation of the relationship between grain size, soil thickness and time (from McKay et al., 1974; Proc. 5th Lunar Sci. Conf., Suppl. 5, Vol. 1, Pergamon).

sand is "driven by the formative process that operate upon it."

To apply Pettijohns (1957) concept to the waterless depositional environment of the lunar soil requires a deeper insight into what we are actually attempting to measure with a maturity index. The answer is simply the total energy expended in the formation of the sediment (Lindsay 1971, 1972c, 1974). The formitive processes operating on the lunar soil in large part relate to the kinetic energy of the meteoroid flux at the lunar surface. Each impact on the lunar surface releases a significant proportion of its kinetic energy in the form of heat energy (Gault and Heitowit, 1963; Braslau, 1970). In turn a proportion of this heat energy is expended in fusing some of the detrital materials excavated by the impact (see Chapter 3). Since the soil is continually reworked by the meteoroid flux the glass content of the soil increases with time (Lindsay, 1971, 1972c, 1975). Thus the amount of glass in some soils could be used as an indicator of soil maturity.

In this light two indices of soil maturity have been proposed. Lindsay (1971) proposed that the total glass-content of the soil is a measure of mineralogic maturity within the confines of Pettijohns (1957) definition. The total glass-content of the soil must increase with time. However, the rate of increase in the glass content will decline exponentially with time as the accumulation rate decreases and more energy is expended in remelting pre-existing glass. The concept was tested using the known radiometric ages of the substrate at different sites, and it was found that soils overlying older substrates contained more glass. When plotted against grain size, however, it was found that soil texture was apparently unrelated to mineralogic maturity suggesting that textural maturity evolves in a more complex manner. In view of the steady-state or cycling stage of soil evolution this is understandable.

In a subsequent definition of maturity McKay et al. (1972) have suggested the use of agglutinates as a maturity index. They found that the agglutinate content of the soil correlates with its exposure age or residence time on the lunar surface. However, the agglutinate content of the soil also correlates with the grain-size parameters, suggesting that it is a measure of textural maturity rather than a measure of total energy (Lindsay, 1974; McKay et al., 1974). In the light of the evolutionary model discussed in the preceding section, it can be seen that agglutinates can only be used as an effective measure of maturity during the agglutination dominated stage of soil devolopment. In the comminution dominated stage agglutinates are not formed whereas in the cycling stage agglutinates are destroyed as fast as they are formed in random excursions away from the "ideal" mature soil. Some of these problems may be overcome if the total agglutinate content of the soil could be evaluated in the way in which Rhodes et al. (1975) have evaluated the agglutinate chemistry.

In summary, the total glass content of the soil must continually increase with time and offer a measure of total energy involved in the development of the soil. The agglutinates offer a more sensitive index of textural maturity during a period of soil development. However, very young or very old soils will not conform to the agglutinate model.

Energy Partitioning and the Flux of Detrital Materials

The energy released by hypervelocity impact at the lunar surface is partitioned in a complex way. First, and possibly most obviously, the kinetic energy of an individual impact event is released through heating and either fusing or vaporizing target and projectile, comminuting the substrate and finally ejecting the heated and comminuted materials. The kinetic energy of the flux is also partitioned in different ways according to the mass spectrum. Different portions of the mass spectrum contribute to or modify the soils in different ways (Fig. 6.2). It is as yet difficult to evaluate these variables but some order of magnitude estimates have been made (Lindsay, 1975).

The post-mare meteoroid flux at the lunar surface produces a primary sediment flux of the order of 2.78 x 10⁻⁷ g cm⁻² yr⁻¹ which represents an erosional efficiency of approximately 1.6 per cent (Gault *et al.*, 1972; Lindsay, 1975). The sediment flux per unit area entering the earth's oceans is 175 times larger than the lunar sediment flux.

Bedrock material appears to be excavated most efficiently by meteoroids larger than 10^3 to 10^4 g. In contrast, agglutination is caused by micrometeoroids in the mass range of 10^{-7} to 10^{-4} g or by about 68 per cent of the flux mass. Layer forming events appear to be the product of meteoroids larger than 7 g or less than 1 per cent of the flux mass.

Despite the tenuous nature of the energy source and the large inefficiencies involved, the meteoroid flux has, over several aeons, produced an extensive dynamic sedimentary body over most of the lunar surface. This sedimentary body probably contains stratigraphic information covering most of the life time of the solar system and perhaps a record of events of galactic magnitude.

References

Adler, I., Trombka, J., Gerard, J., Lowman, P., Schmadebeck, R., Blodgeth, H., Eller, E., Yin, L., Lamothe, R., Gorenstein, P. and Bjorkholm, P., 1972a. Apollo 15 geochemical X-ray fluorescence experiments. Preliminary report. Science, 175: 436-440.

- Adler, I., Trombka, J., Gerard, J., Lowman, P., Schmadebeck, R., Blodgeth, H., Eller, E., Yin, L., Lamothe, R., Gorenstein, P., Bjorkholm, P., Gursky, H., Harris, B., Golub, L. and Harnden, R. F., 1972b. X-ray fluorescence experiment. In: Apollo 16 Preliminary Science Report, NASA SP- 315, 19-1 to 19-14.
- Apollo Soil Survey, 1971. Apollo 14: nature and origin of rock types in soil from the Fra Mauro Formation. Earth Planet. Sci. Lett., 12: 49-54.
- Arrhenius, G., Liang, S., Macdougall, D., Wilkening, L., Bhandari, N., Blat, S., Lal, D., Rajagopalan, G., Tamhane, A. S. and Benkatavaradan, V. S., 1971. The exposure history of the Apollo 12 regolith. Proc. Second Lunar Sci. Conf., Suppl. 2, Geochim. Cosmochim. Acta, 3: 2583-2598.
- Apollo Soil Survey, 1974. Phase chemistry of Apollo 14 soil sample 14259. Modern Geol., 5: 1-13.
- Braslau, D., 1970. Partitioning of energy in hypervelocity impact against loose sand targets. Jour. Geophys. Res., 75: 3987-3999.
- Butler, J. C., Greene, G. M. and King, E. A., 1973. Grain size frequency distributions and modal analyses of Apollo 16 fines. Proc. Fourth Lunar Sci. Conf., Suppl. 4, Geochim. Cosmochim. Acta, 1: 267-278.
- Butler, J. C. and King, E. A., 1974. Analysis of the grain size-frequency distributions of lunar fines. Proc. Fifth Lunar Sci. Conf., Suppl. 5, Geochim. Cosmochim. Acta, 3: 829-841.
- Carrier, W. D., Mitchell, J. K., and Mahmood, A., 1974. Lunar soil density and porosity. Proc. Fifth Lunar Sci. Conf., Suppl. 5, Geochim. Cosmochim. Acta, 3: 2361-2364.
- Chao, E. T. C., Boreman, J. A., Minkin, J. A., James, O. B. and Desborough, G. A., 1970. Lunar glasses of impact origin: physical and chemical characteristics and geologic implications. *Jour. Geophys. Res.*, 75: 7445-7479.
- Cherkasov, I. I., Vakhnin, V. M., Kemurjian, A. L., Mikhailov, L. N., Mikheyev, V. V., Musatov, A. A., Smorodinov, M. J. and Shvarey, V. V., 1968. Determination of physical and mechanical properties of the lunar surface layer by means of Luna 13 automatic station: Tenth Plenary Meeting, COSPAR, London.
- Christensen, E. M., Batterson, S. A., Benson, H. E., Choate, R., Jaffe, L. D., Jones, R. H., Ko, H. Y., Spencer, R. L., Sperling, F. B. and Sutton, G. H., 1967. Lunar surface mechanical properties: Surveyor III Mission Report, Part II, Scientific Results: California Inst. Technology Jet Propulsion Lab. Tech. Rept. 82-1177, 111-153.
- Cooper, M. R., Kovach, R. L., and Watkins, J. S., 1974. Lunar near-surface structure. Rev. Geophys. Space Phys., 12: 291-308.
- Duke, M. B., Woo, C. C., Sellers, G. A., Bird, M. L. and Finkelman, R. B., 1970. Genesis of soil at Tranquillity Base. Proc. Apollo 11 Lunar Sci. Conf., Suppl. 1, Geochim. Cosmochim. Acta, 1: 347-361.
- Duke, M. B. and Nagel, J. S., 1975. Stratification in the lunar regolith a preliminary view. The Moon, 13: 143-158.
- Englehardt, W. von, Arndt, J. and Schneider, H., 1973. Apollo 15: evolution of the regolith and origin of glasses. Proc. Fourth Lunar Sci. Conf., Suppl. 4, Geochim. Cosmochim. Acta, 1: 239-249.
- Epstein, B., 1947. The mathematical description of certain breakage mechanisms leading to the logarithmic-normal distribution. *Jour. Franklin Inst.*, 44: 471-477.
- Finkelman, R. B., 1973. Analysis of the ultrafine fraction of the Apollo 14 regolith. Proc. Fourth Lunar Sci. Conf., Suppl. 4, Geochim. Cosmochim. Acta, 1: 179-189.
- Fredricksson, K., Brenner, P., Nelen, J., Noonan, A., Dube, A. and Reid, A., 1974. Comparitive studies of impact glasses and breccias. *Lunar Science-V*, The Lunar Science Inst., Houston, Texas, 245-247.
- Friedman, G. M., 1958. Determination of sieve-size distribution from thin-section data for sedimentary petrological studies. *Jour. Geology*, 66: 394-416.

Friedman, G. M., 1962. Comparison of moment measures for sieving and thin-section data in sedimentary petrographic studies. Jour. Sediment. Pet., 32: 15-25.

- Fulchignoni, M., Funiciello, R., Taddeucci, A. and Trigila, R., 1971. Glassy spheroids in lunar fines from Apollo 12 samples 12070,37; 12001,73; and 12057,60. Proc. Second Lunar Sci. Conf., Suppl. 2, Geochim. Cosmochim. Acta, 1: 937-948.
- Heiken, G. H., McKay, D. S. and Fruland, R. M., 1973. Apollo 16 soils: grain size analyses and petrography. Proc. Fourth Lunar Sci. Conf., Suppl. 4, Geochim. Cosmochim. Acta, 1: 251-265.
- Gault, D. E., Quaide, W. L., Oberbeck, V. R., and Moore, H. J., 1966. Lunar 9 photographs: evidence for a fragmental surface layer. Science. 153: 985-988.
- Gault, D. E. and Heitowit, E. D., 1963. The partitioning of energy for hypervelocity impact craters formed in rock. Proc. Sixth Hypervelocity Impact Symp., Cleveland, Ohio, 2: 419-456.
- Gault, D. E., Horz, F., and Hartung, J. B., 1972. Effects of microcratering on the lunar surface. Proc. Third Lunar Sci. Conf., Suppl. 3, Geochim. Cosmochim. Acta, 3: 2713-2734.
- Gault. D. E., Horz, F., Brownlee, D. E. and Hartung, J. B., 1974. Mixing of the lunar regolith. Proc. Fifth Lunar Sci. Conf., Suppl. 5, Geochim. Cosmochim. Acta, 3: 2365-2386.
- Gibbons, R. V., Morris, R. V., Horz, F. and Thompson, T. D., 1975. Petrographic and ferromagnetic resonance studies of experimentally shocked regolith analogues. Proc. Sixth Lunar Sci. Conf., Geochim. Cosmochim. Acta, (in press).
- Goldstein, J. I., Axon, H. J. and Yen, C. F., 1972. Metallic particles in Apollo 14 lunar soils. Proc. Third Lunar Sci. Conf., Suppl. 3, Geochim. Cosmochim. Acta, 1: 1037-1064.
- Goles, G. G., Duncan, A. R., Lindstrom, D. J., Martin, M. R., Beyer, R. L., Osawa, M., Randle, K., Meek, L. T., Steinborn, T. L. and McKay, S. M., 1971. Analyses of Apollo 12 specimens: compositional variations, differentiation processes, and lunar soil mixing models. Proc. Second Lunar Sci. Conf., Suppl. 2, Geochim. Cosmochim. Acta, 2: 1063-1081.
- Gose, W. A., Pearce, G. W. and Lindsay, J. F., 1975. Magnetic stratigraphy of the Apollo 15 deep drill core. Proc. Sixth Lunar Sci. Conf., Suppl. 6, Geochim. Cosmochim. Acta, (in press).
- Green, D. H., Ringwood, A. E., Ware, N. G., Hibberson, W. O., Major, H. and Kiss, E., 1971. Experimental petrology and petrogenesis of Apollo 12 basalts. Proc. Second Lunar Sci. Conf., Suppl. 2, Geochim. Cosmochim. Acta, 1: 601-615.
- Halmos, P. R., 1944. Random alms. Ann. Math. Stat., 15: 182-189.
- Heiken, G., Duke, M., Fryxell, R., Nagle, S., Scott, R. and Sellers, G., 1972. Stratigraphy of the Apollo 15 drill core. NASA TMX-58101, 21 pp.
- Hodges, F. N. and Kushiro, I., 1973. Petrology of Apollo 16 lunar highland rocks. Proc. Fourth Lunar Sci. Conf., Suppl. 4, Geochim. Cosmochim. Acta, 1: 1033-1048.
- Hubbard, N., Meyer, C., Gast, P. and Wiesmann, H., 1971. The composition and derivation of Apollo 12 soils. Earth Planet. Sci. Lett., 10: 341-350.
- King, E. A., Butler, J. C. and Carman, M. F., 1971. The lunar regolith as sampled by Apollo 11 and 12; grain size analyses, and modal amalyses, origins of particles. Proc. Second Lunar Sci. Conf., Suppl. 2, Geochim. Cosmochim. Acta, 1: 737-746.
- King, E. A., Butler, J. C. and Carman, M. F., 1972. Chondrules in Apollo 14 samples and size analyses of Apollo 14 and 15 fines. Proc. Third Lunar Sci. Conf., Suppl_3, Geochim. Cosmochim. Acta, 1: 673-686.
- Kolmogoroff, A. N., 1941. Uber das logarithmisch normale verteilungsgesetz der dimensionen der teilchen bel zerstuchelung. Akad. Nauk SSSR, Doklady, 31: 99-101.
- Lindsay, J. F., 1971a. Sedimentology of Apollo 11 and 12 lunar soil. Jour. Sediment. Pet., 41: 780-797.
- Lindsay, J. F., 1971b. Mixing models and the recognition of end-member groups in Apollo 11 and 12 soils. Earth Planet. Sci. Lett., 12: 67-72.
- Lindsay, J. F., 1972a. Sedimentology of clastic rocks from the Fra Mauro region of the moon. Jour. Sediment. Pet., 42: 19-32.
- Lindsay, J. F., 1972b. Sedimentology of clastic rocks returned from the moon by Apollo 15. Geol. Soc. Amer. Bull., 83: 2957-2970.
- Lindsay, J. F., 1972c. Development of soil on the lunar surface. Jour. Sediment. Pet., 42: 876-888.

Lindsay, J. F., 1973. Evolution of lunar grain-size and shape parameters. Proc. Fourth Lunar Sci. Conf., Suppl. 4, Geochim. Cosmochim. Acta, 1: 215-224.

- Lindsay, J. F., 1974. Transportation of detrital materials on the lunar surface: evidence from Apollo 15. Sedimentology, 21: 323-328.
- Lindsay, J. F., 1975. A steady state model for the lunar soil. Geol. Soc. Amer. Bull., 86: 1661-1670. Lindsay, J. F. and Srnka, L. J., 1975. Galactic dust lanes and the lunar soil. Nature, 257: 776-778.
- Lindsay, J. F., Heiken, G. H. and Fryxell, R., 1971. Description of core samples returned by Apollo 12. NASA TMX-58066, 19 pp.
- McKay, D. S. and Morrison, D. A., 1971. Lunar breccia. Jour. Geophys. Res., 76: 5658-5669.
- McKay, D. S., Greenwood, W. R., and Morrison, D. A., 1970. Origin of small lunar particles and breccia from the Apollo 11 site. Proc. Apollo 11 Lunar Sci. Conf., Suppl. 1, Geochim. Cosmochim. Acta, 1: 673-693.
- McKay, D. S., Morrison, D. A., Clanton, U. S., Ladle, G. H. and Lindsay, J. F., 1971. Apollo 12 soil and breccia. Proc. Second Lunar Sci. Conf., Suppl. 2, Geochim. Cosmochim. Acta, 1: 755-773.
- McKay, D. S., Heiken, G. H., Taylor, R. M., Clanton, U. S. and Morrison, D. A., 1971. Apollo 14 soils. size distribution and particle types. Proc. Third Lunar Sci. Conf., Suppl. 3, Geochim Cosmochim. Acta, 1: 983-994.
- McKay, D. S., Fruland, R. M. and Heiken, G. H., 1974. Grain size and the evolution of lunar soils. Proc. Fifth Lunar Sci. Conf., Suppl. 5, Geochim. Cosmochim. Acta, 1: 887-906.
- Meyer, C., Brett, R., Hubbard, N., Morrison, D., McKay, D., Aitken, F., Takeda, H. and Schonfeld, E., 1971. The mineralogy chemistry and origin of the KREEP component in soil samples from the Ocean of Storms. Proc. Second Lunar Sci. Conf., Suppl. 2, Geochim. Cosmochim. Acta, 1: 393-411.
- Moore, J. G. and Peck, D. L., 1962. Accretionary lapilli in volcanic rocks of the western continental United States. Jour. Geol., 70: 182-193.
- Nakamura, Y., Dorman, J., Duennebier, F., Lammlein, D., and Latham, G., 1975. Shallow lunar structure determined from the passive seismic experiment. The Moon, 13: 57-66.
- Oberbeck, V. R., and Quaide, W. L., 1967. Estimated thickness of a fragmental surface layer of Oceanus Procellarum. *Jour. Geophys. Res.*, 72: 4697-4704.
- Oberbeck, V. R. and Quaide, W. L., 1968. Genetic implications of lunar regolith thickness variations. Icarus, 9: 446-465.
- Pettijohn, F. J., 1957. Sedimentary Rocks. Harper and Rowe, N. Y., 2nd Ed., 718 pp.
- Quaide, W. L. and Oberbeck, V. R., 1968. Thickness determinations of the lunar surface layer from lunar impact craters. Jour. Geophys. Res., 73: 5247-5270.
- Quaide, W. L. and Oberbeck, V. R., 1975. Development of mare regolith: some model implications... The Moon, 13: 27-55.
- Reid, A. M., 1974. Rock types present in lunar highland soils. The Moon, 9: 141-146.
- Reid, A. M., Warner, J., Ridley, W. I., Johnston, D. A., Harmon, R. S., Jakes, P. and Brown, R. W., 1972a. The major element compositions of lunar rocks as inferred from glass compositions in the lunar soils. Proc. Third Lunar Sci. Conf., Suppl. 3, Geochim. Cosmochim. Acta, 1: 379-399.
- Reid, A. M., Warner, J., Ridley, W. I., and Brown, R. W., 1972b. Major element composition of glasses in three Apollo 15 soils. Meteoritics, 7:395-415.
- Rennilson, J. J., Dragg, J. L., Morris, E. C., Shoemaker, E. M. and Turkevich, A., 1966. Lunar surface topography. Surveyor I Mission Report, Part 2 Scientific Data and Results, Jet Propulsion Lab. Tech. Rept. 82-1023.
- Rhodes, J. M., Rodgers, K. V., Shih, C., Bansal, B. M., Nyquist, L. E., Wiesmann, H., and Jubbard, N. J., 1974. The relationship between geology and soil chemistry at the Apollo 17 landing site. Proc. Fifth Lunar Sci. Conf., Suppl. 5, Geochim. Cosmochim. Acta, 2: 1097-1117.
- Rhodes, J. M., Adams, J. B., Blanchard, D. P., Charette, M. P., Rodgers, K. V., Jocogs, J. W., Brannon, J. C. and Haskin, L. A., 1975. Chemistry of agglutinate fractions in lunar soils. Proc. Sixth Lunar Sci. Conf., Suppl. 6, Geochim. Cosmochim. Acta, (in press).
- Ridley, W. I., Reid, A. M., Warner, J. L., Brown, R. W., Gooley, R. and Donaldson, C., 1973. Glass compositions in Apollo 16 soils 60501 and 61221. Proc. Fourth Lunar Sci. Conf., Suppl. 4, Geochim. Cosmochim. Acta, 1: 309-321.

Ringwood, A. E. and Essene, E., 1970. Petrogenesis of Apollo 11 basalts, internal constitution and origin of the moon. Proc. Apollo 11 Lunar Sci. Conf., Suppl. 1, Geochim. Cosmochim. Acta, 1: 769-799.

- Schonfeld, E. and Meyer, C., 1972. The abundances of components of the lunar soils by a least-squares mixing model and the formation age of KREEP. Proc. Third Lunar Sci. Conf., Suppl. 3, Geochim. Cosmochim. Acta. 2: 1397-1420.
- Scott, R. F. and Robertson, F. I., 1967. Soil mechanics surface samples; Lunar surface tests, results and analyses: Surveyor III Mission Report, Part II, Scientific Results. Jet Propulsion Lab. Tech. Rept. 82-1177. 69-110.
- Shoemaker, E. M., Batson, R. M., Holt, H. E., Morris, E. C., Rennilson, J. J. and Whitaker, E. A., 1967. Television observations for Surveyor III: Surveyor III Mission Report, Part II, Scientific Results. Jet Propulsion Lab. Tech. Rept. 82-1177, 9-67.
- Shoemaker, E. M., Hait, M. H., Swann, G. A., Schleicter, D. L., Schaber, G. G., Sutton, R. L., Dahlem, D. H., Goddard, E. N. and Waters, A. C., 1970. Origin of the lunar regolith at Tranquility Base. Proc. Apollo 11 Lunar Sci. Conf., Suppl. 1, Geochim. Cosmochim, Acta, 3: 2399-2412.
- Simonds, C. H., 1973. Sintering and hot pressing of Fra Mauro composition glass and the lithification of lunar breccias. Am. Jour. Sci., 273: 428-439.
- Taylor, S. R., 1975. Lunar Science: A Post-Apollo View. Pergamon Press, N. Y., 372 pp.
- Turkevich, A. L., 1973a. The average chemical composition of the lunar surface. Proc. Fourth Lunar Sci. Conf., Suppl. 4, Geochim. Cosmochim. Acta, 2: 1159-1168.
- Turkevich, A. L., 1973b. Average chemical composition of the lunar surface. The Moon, 8: 365-367.
- Uhlmann, D. R., Klein, L. and Hopper, R. W., 1975. Sintering, crystallization, and breccia formation. The Moon, 13: 277-284.
- Walker, D., Grove, T. L., Longhi, J., Stolper, E. M. and Hays, J. F., 1973. Origin of lunar feldspathic rocks. Earth Planet. Sci. Lett., 20: 325-336.
- Waters, A. C., Fisher, R. V., Garrison, R. E. and Wax, D., 1971. Matrix characteristics and origin of lunar breccia samples no. 12034 and 12037. Proc. Second Lunar Sci. Conf., Suppl. 2, Geochim. Cosmochim. Acta, 1: 893-907.
- Watkins, J. S. and Kovach, R. L., 1973. Seismic investigations of the lunar regolith. Proc. Fourth Lunar Sci. Conf., Suppl. 4, Geochim, Cosmochim, Acta, 3: 2561-2574.
- Wood, J. A., Dickey, J. S., Marvin, U. B. and Powell, B. N., 1970. Lunar anorthosites and a geophysical model of the moon. Proc. Apollo 11 Lunar Sci. Conf., Suppl. 1, Geochim. Cosmochim. Acta, 1: 965-988.